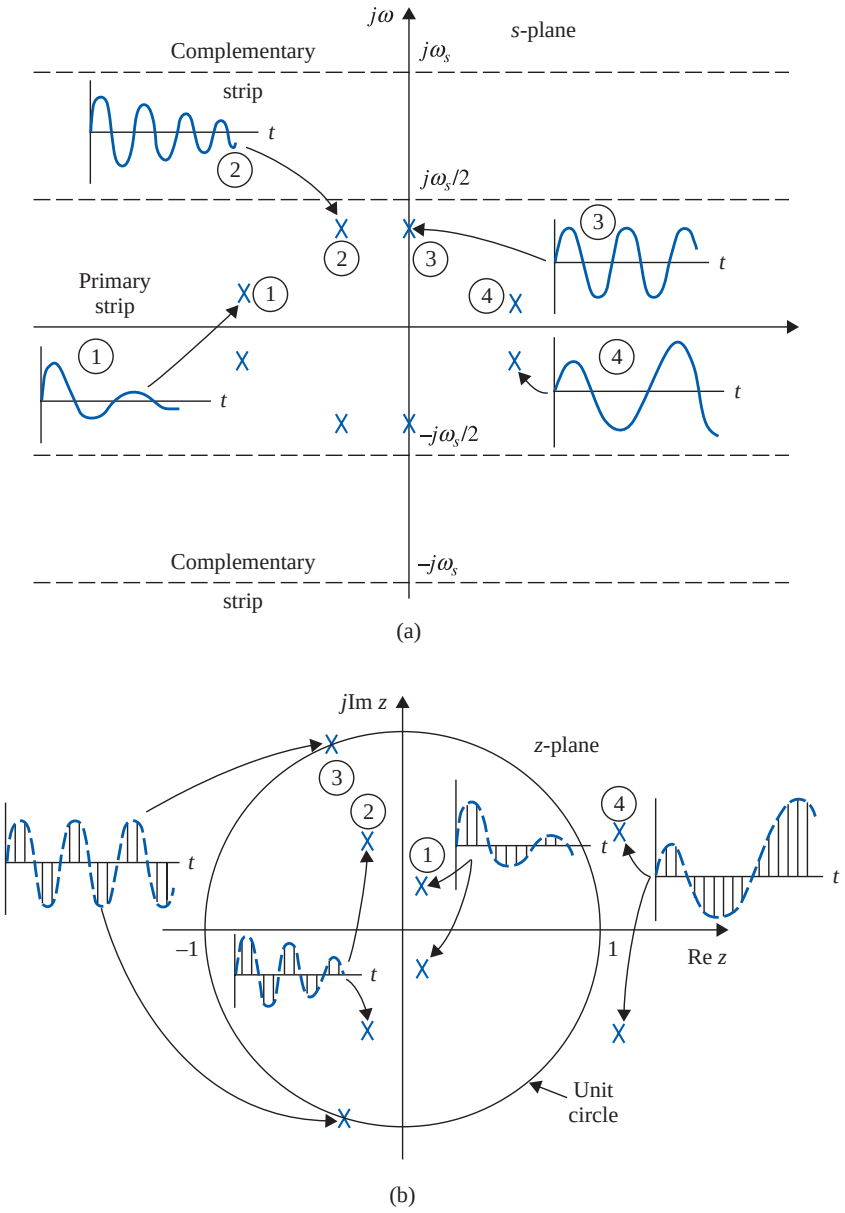

Figure H-27 (a) Transient responses corresponding to various pole locations of $Y^*(s)$ in the s-plane (complex-conjugate poles only). (b) Transient-response sequence corresponding to various pole locations of $Y(z)$ in the z-plane.

Thus, the output sequence will occur in alternating positive and negative pulses, as shown in Fig. H-28(b).

Complex-Conjugate Roots in the z-Plane: Complex-conjugate roots inside the unit circle in the z-plane correspond to oscillatory responses that decay with an increase in kT. Roots that are closer to the unit circle will decay slower. As the roots move toward the second and the third quadrants, the frequency of oscillation of the response increases. Refer to Figs. H-27 and H-28 for typical examples.

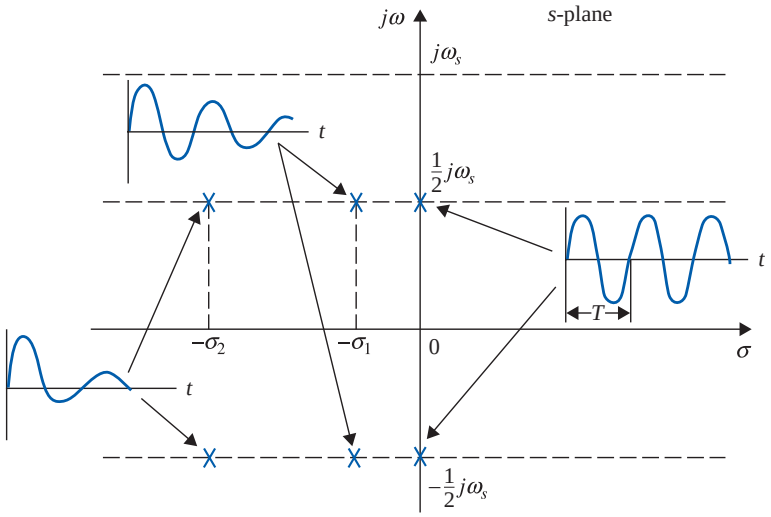

(a)

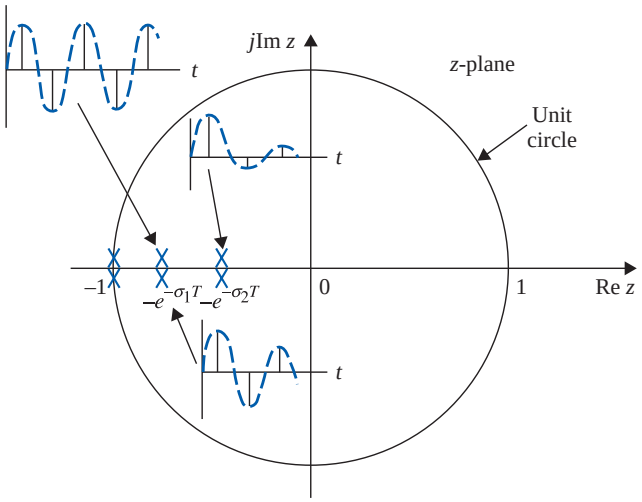

(b)

Figure H-28 (a) Transient responses corresponding to various pole locations of $Y^*(s)$ in the s-plane (complex-conjugate poles on the boundaries between periodic strips). (b) Transient-response sequence corresponding to various pole locations of $Y(z)$ in the z-plane.

▶ H-7 STEADY-STATE ERROR ANALYSIS OF DISCRETE-DATA CONTROL SYSTEMS

Because the input and output signals of a typical discrete-data control system are continuous-time functions, as shown in the block diagram of Fig. H-19, the error signal should still be defined as

$$e(t) = r(t) - y(t) \tag{H-195}$$

where $r(t)$ is the input and $y(t)$ is the output. The error analysis conducted here is only for unity-feedback systems with $H(s) = 1$. Due to the discrete data that appear inside the system, z-transform or difference equations are often used, so that the input and output are

represented in sampled form, $r(kT)$ and $y(kT)$, respectively. Thus, the error signal is more appropriately represented by $e^*(t)$ or $e(kT)$. That is,

$$e^*(t) = r^*(t) - y^*(t) \tag{H-196}$$

or

$$e(kT) = r(kT) - y(kT) \tag{H-197}$$

The steady-state error at the sampling instants is defined as

$$e_{ss}^* = \lim_{k \to \infty} e^*(t) = \lim_{k \to \infty} e(kT) \tag{H-198}$$

By using the final-value theorem of the z-transform, the steady-state error is

$$e_{ss}^* = \lim_{k \to \infty} e^*(kT) = \lim_{z \to 1} \left(1 - z^{-1}\right) E(z) \tag{H-199}$$

provided that the function $(1 - z^{-1})E(z)$ does not have any pole on or outside the unit circle in the z-plane. It should be pointed out that, because the true error of the system is $e(t)$, e_{ss}^* predicts only the steady-state error of the system at the sampling instants.

By expressing $E(z)$ in terms of $R(z)$ and $G_{ho}G_p(z)$, Eq. (H-199) is written

$$e_{ss}^* = \lim_{k \to \infty} e(kT) = \lim_{z \to 1} \left(1 - z^{-1}\right) \frac{R(z)}{1 + G_{ho}G_p(z)} \tag{H-200}$$

This expression shows that the steady-state error depends on the reference input $R(z)$ as well as the forward-path transfer function $G_{ho}G_p(z)$. Just as in the continuous-data systems, we shall consider only the three basic types of input signals and the associated error constants and relate e_{ss}^* to these and the type of the system.

Let the transfer function of the controlled process in the system of Fig. H-18 be of the form

$$G_p(s) = \frac{K(1 + T_a s)(1 + T_b s) \cdots (1 + T_m s)}{s^j (1 + T_1 s)(1 + T_2 s) \cdots (1 + T_n s)} \tag{H-201}$$

where $j = 0, 1, 2, \ldots$. The transfer function $G_{ho}G_p(z)$ is

$$G_{h0}G_p(z) = \left(1 - z^{-1}\right) \mathcal{Z} \left[\frac{K(1 + T_a s)(1 + T_b s) \cdots (1 + T_m s)}{s^{j+1} (1 + T_1 s)(1 + T_2 s) \cdots (1 + T_n s)} \right] \tag{H-202}$$

Steady-State Error Due to a Step-Function Input

When the input to the system, $r(t)$, in Fig. H-18 is a step function with magnitude R, the z-transform of $r(t)$ is

$$R(z) = \frac{Rz}{z - 1} \tag{H-203}$$

Substituting $R(z)$ into Eq. (H-200), we get

$$e_{ss}^* = \lim_{z \to 1} \frac{R}{1 + G_{ho}G_p(z)} = \frac{R}{1 + \lim_{z \to 1} G_{ho}G_p(z)} \tag{H-204}$$

Let the **step-error constant** be defined as

$$K_p^* = \lim_{z \to 1} G_{ho}G_p(z) \tag{H-205}$$

Eq. (H-204) becomes

$$e_{ss}^* = \frac{R}{1 + K_p^*} \tag{H-206}$$

Thus, we see that the steady-state error of the discrete-data control system in Fig. H-18 is related to the step-error constant K_p^* in the same way as in the continuous-data case, except that K_p^* is given by Eq. (H-205).

We can relate K_p^* to the system type as follows.

For a type-0 system, $j = 0$ in Eq. (H-202), and the equation becomes

$$G_{ho}G_p(z) = \left(1 - z^{-1}\right)\mathcal{Z}\left[\frac{K(1 + T_a s)(1 + T_b s)\cdots(1 + T_m s)}{s(1 + T_1 s)(1 + T_2 s)\cdots(1 + T_n s)}\right] \tag{H-207}$$

Performing partial-fraction expansion to the function inside the square brackets of the last equation, we get

$$\begin{aligned} G_{ho}G_p(z) &= \left(1 - z^{-1}\right)\mathcal{Z}\left[\frac{K}{s} + \text{terms due to the nonzero poles}\right] \\ &= \left(1 - z^{-1}\right)\left[\frac{Kz}{z - 1} + \text{terms due to the nonzero poles}\right] \end{aligned} \tag{H-208}$$

Because the terms due to the nonzero poles do not contain the term $(z - 1)$ in the denominator, the step-error constant is written

$$K_p^* = \lim_{z \to 1} G_{ho}G_p(z) = \lim_{z \to 1}\left(1 - z^{-1}\right)\frac{Kz}{z - 1} = K \tag{H-209}$$

Similarly, for a type-1 system, $G_{ho}G_p(z)$ will have an s^2 term in the denominator that corresponds to a term $(z - 1)^2$. This causes the step-error constant $K_p^*$to be infinite. The same is true for any system type greater than 1. The summary of the error constants and the steady-state error due to a step input is as follows:

System Type	K_p^*	e_{ss}^*
0	K	$R/(1 + K)$
1	∞	0
2	∞	0

Steady-State Error Due to a Ramp-Function Input

When the reference input to the system in Fig. H-18 is a ramp function of magnitude R, $r(t) = Rtu_s(t)$. The steady-state error in Eq. (H-200) becomes

$$e_{ss}^* = \lim_{z \to 1} \frac{RT}{(z - 1)\left[1 + G_{ho}G_p(z)\right]} = \frac{R}{\lim\limits_{z \to 1} \dfrac{z - 1}{T} G_{ho}G_p(z)} \tag{H-210}$$

Let the **ramp-error constant** be defined as

$$K_v^* = \frac{1}{T}\lim_{z \to 1}\left[(z - 1)G_{ho}G_p(z)\right] \tag{H-211}$$

Then, Eq. (H-210) becomes

$$e_{ss}^* = \frac{R}{K_v^*} \tag{H-212}$$

The ramp-error constant K_v^* is meaningful only when the input $r(t)$ is a ramp function and if the function $(z-1)G_{ho}G_p(z)$ in Eq. (H-211) does not have any poles on or outside the unit circle $|z| = 1$. The relations among the steady-state error e_{ss}^*, K_v^*, and the system type when the input is a ramp function with magnitude R are summarized as follows.

System Type	K_v^*	e_{ss}^*
0	0	∞
1	K	R/K
2	∞	0

Steady-State Error Due to a Parabolic-Function Input

When the input is a parabolic function, $r(t) = Rtu_s(t)/2$; the z-transform of $r(t)$ is

$$R(z) = \frac{RT^2 z(z+1)}{2(z-1)^3} \tag{H-213}$$

From Eq. (H-200), the steady-state error at the sampling instants is

$$\begin{aligned} e_{ss}^* &= \frac{T^2}{2} \lim_{z \to 1} \frac{R(z+1)}{(z-1)^2 \left[1 + G_{ho}G_p(z)\right]} \\ &= \frac{R}{\frac{1}{T^2} \lim_{z \to 1} (z-1)^2 G_{ho}G_p(z)} \end{aligned} \tag{H-214}$$

By defining the **parabolic-error constant** as

$$K_a^* = \frac{1}{T^2} \lim_{z \to 1} \left[(z-1)^2 G_{ho}G_p(z)\right] \tag{H-215}$$

the steady-state error due to a parabolic-function input is

$$e_{ss}^* = \frac{R}{K_a^*} \tag{H-216}$$

The relations among the steady-state error e_{ss}^*, K_a^*, and the system type when the input is a parabolic function with its z-transform described by Eq. (H-213) are summarized as follows.

System Type	K_a^*	e_{ss}^*
0	0	∞
1	0	∞
2	K	R/K
3	∞	0

▶ H-8 ROOT LOCI OF DISCRETE-DATA SYSTEMS

The root-locus technique can be applied to discrete-data systems without any complications. With the z-transformed transfer function, the root loci for discrete-data systems are plotted in the z-plane, rather than in the s-plane. Let us consider the discrete-data control system shown in Fig. H-29. The characteristic equation roots of the system satisfy the following equation:

$$1 + GH^*(s) = 0 \tag{H-217}$$

in the s-plane, or

$$1 + GH(z) = 0 \tag{H-218}$$

in the z-plane. From Eq. (H-64), $GH^*(s)$ is written

$$GH^*(s) = \frac{1}{T}\sum_{n=-\infty}^{\infty} G(s + jn\omega_s)H(s + jn\omega_s) \tag{H-219}$$

which is an infinite series. Thus, the poles and zeros of $GH^*(s)$ in the s-plane will be infinite in number. This evidently makes the construction of the root loci of Eq. (H-217) in the s-plane quite complex. As an illustration, consider that, for the system of Fig. H-29,

$$G(s)H(s) = \frac{K}{s(s+1)} \tag{H-220}$$

Substituting Eq. (H-220) into Eq. (H-219), we get

$$GH^*(s) = \frac{1}{T}\sum_{n=-\infty}^{\infty} \frac{K}{(s + jn\omega_s)(s + jn\omega_s + 1)} \tag{H-221}$$

which has poles at $s = -jn\omega_s$ and $s = -1 - jn\omega_s$, where n takes on all integers between $-\infty$ and ∞. The pole configuration of $GH^*(s)$ is shown in Fig. H-30(a). By using the properties of the RL in the s-plane, RL of $1 + GH^*(s) = 0$ are drawn as shown in Fig. H-30(b) for the sampling period $T = 1$ s. The RL contain an infinite number of branches, and these clearly indicate that the closed-loop system is unstable for all values of K greater than 4.32. In contrast, it is well known that the same system without sampling is stable for all positive values of K.

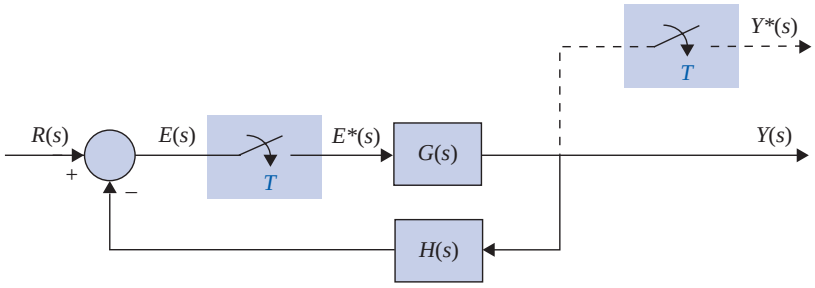

Figure H-29 Discrete-data control system.

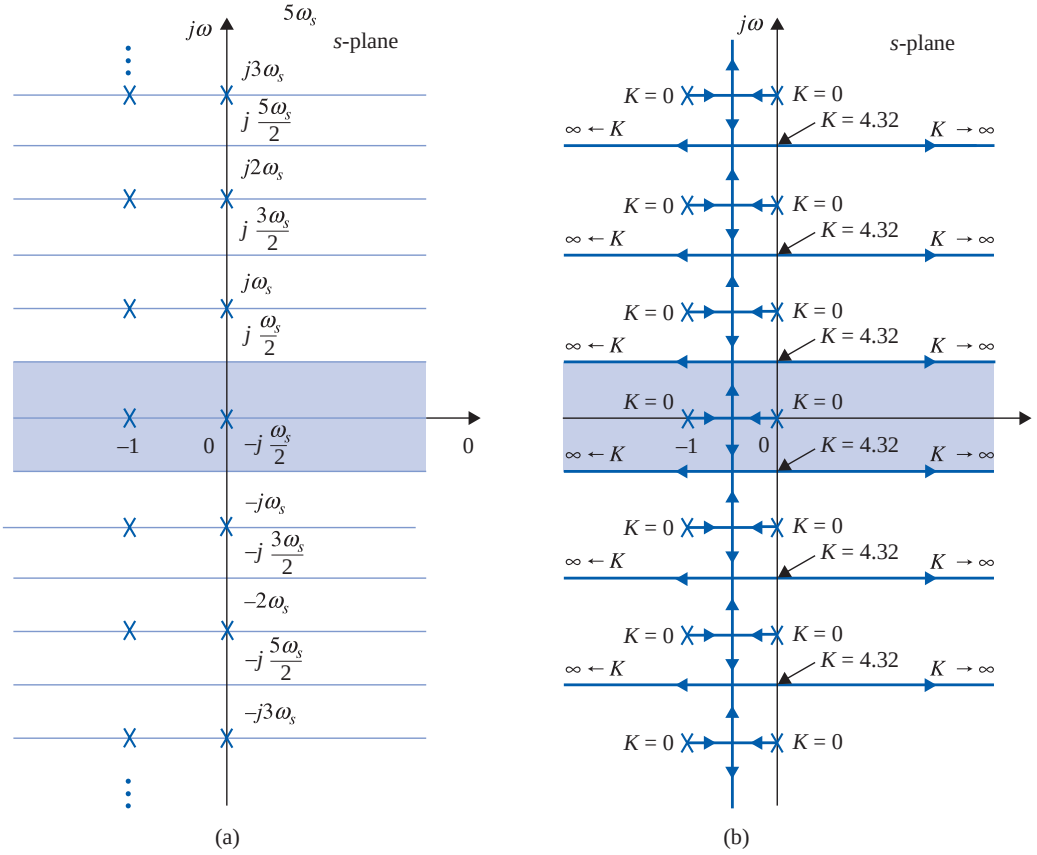

Figure H-30 Pole configuration of $GH*(s)$ and the root-locus diagram in the s-plane for the discrete-data system in Fig. H-29 with $G(s)H(s) = \dfrac{K}{s(s+1)}$, $T = 1$ sec.

The root-locus problem for discrete-data systems is simplified if the root loci are constructed in the z-plane using Eq. (H-218). Because Eq. (H-218) is, in general, a rational function in z with constant coefficients, its poles and zeros are finite in number, and the number of root loci is finite in the z-plane. The same procedures of construction for continuous-data systems are directly applicable in the z-plane for discrete-data systems. The following examples illustrate the constructions of root loci for discrete-data systems in the z-plane.

▶ EXAMPLE H-8-1 Consider that for the discrete-data system shown in Fig. H-29 the loop transfer function in the z domain is

$$GH(z) = \frac{0.632Kz}{(z-1)(z-0.368)} \tag{H-222}$$

The RL of the closed-loop characteristic equation are constructed based on the pole–zero configuration of $GH(z)$, as shown in Fig. H-31. Notice that, when the value of K exceeds 4.32, one of the two roots moves outside the unit circle, and the system becomes unstable. The constant-damping-ratio locus may be superimposed on the RL to determine the required value of K for a specified damping ratio. In Fig. H-31, the constant-damping-ratio locus for $\zeta = 0.5$ is drawn, and the intersection with the RL gives the desired value of $K = 1$. For the same system, if the sampling period T is increased to 2 seconds, the z-transform loop transfer function becomes

$$GH(z) = \frac{0.865Kz}{(z-1)(z-0.135)} \tag{H-223}$$

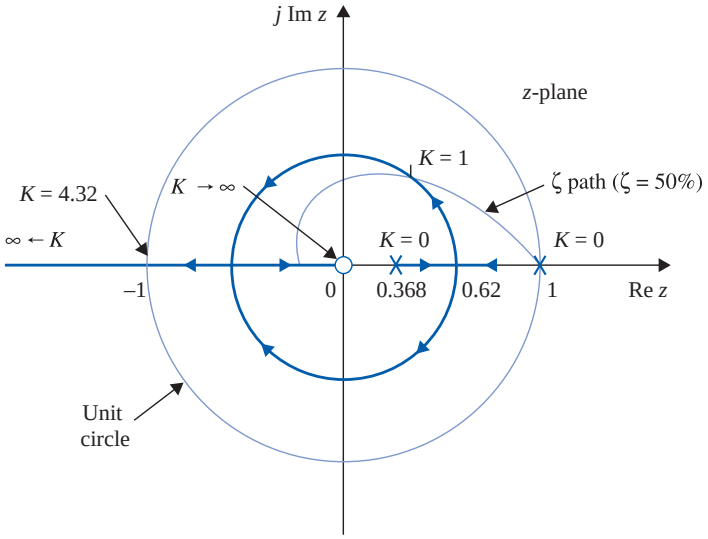

Figure H-31 Root-locus diagram of a discrete-data control system without zero-order-hold. $G(s)H(s) = \dfrac{K}{s(s+1)}$, $T = 1$ second.

The RL for this case are shown in Fig. H-32. Note that, although the complex part of the RL for $T = 2$ seconds takes the form of a smaller circle than that when $T = 1$ second, the system is actually less stable, because the marginal value of K for stability is 2.624, as compared with the marginal K of 4.32 for $T = 1$ second.

Next, let us consider that a zero-order-hold is inserted between the sampler and the controlled process $G(s)$ in the system of Fig. H-29. The loop transfer function of the system with the zero-order-hold is

$$G_{ho}GH(z) = \frac{K\left[(T - 1 + e^{-T})z - Te^{-T} + 1 - e^{-T}\right]}{(z-1)(z-e^{-T})} \tag{H-224}$$

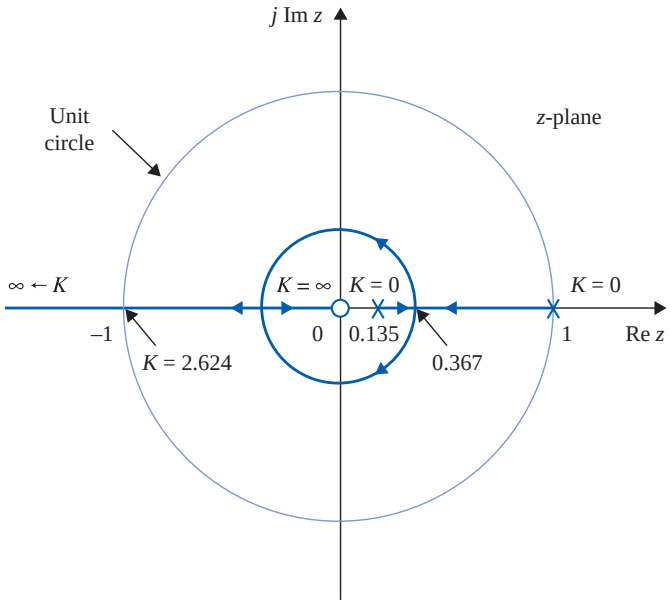

Figure H-32 Root-locus diagram of a discrete-data control system without zero-order-hold. $G(s)H(s) = \dfrac{K}{s(s+1)}$, $T = 2$ seconds.

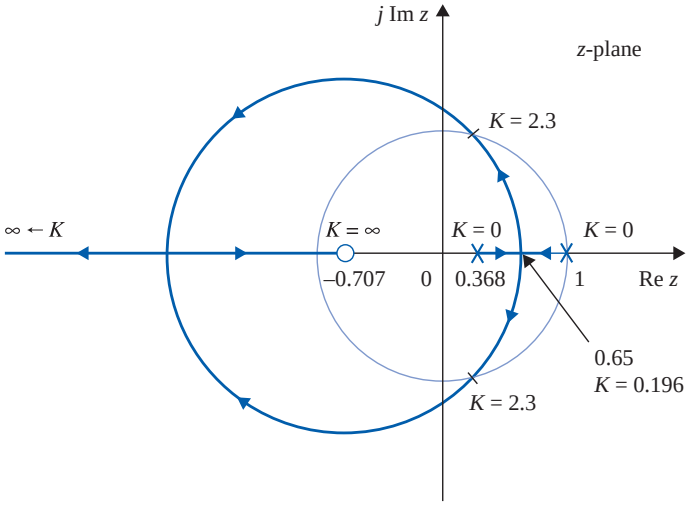

(a) Root loci for $T = 1$ second

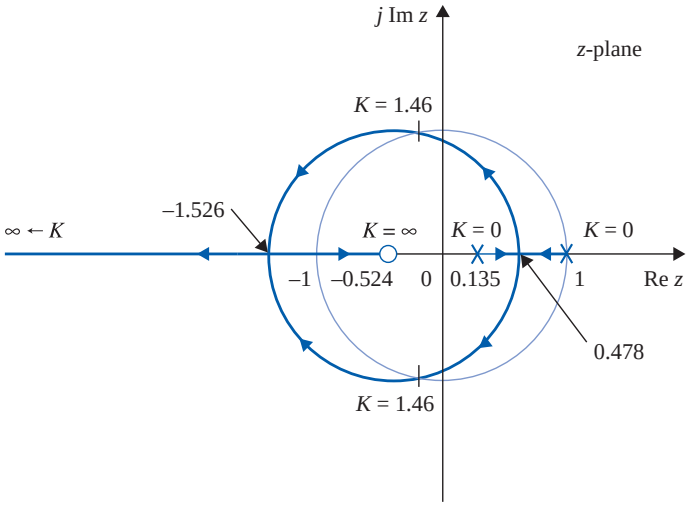

(b) Root loci for $T = 2$ seconds

Figure H-33 Root-locus diagram of a discrete-data control system with zero-order-hold. $G(s)H(s) = \dfrac{K}{s(s+1)}$.

The RL of the system with ZOH for $T = 1$ and 2 seconds are shown in Fig. H-33(a) and H-33(b), respectively. In this case, the marginal value of stability for K is 2.3 for $T = 1$ second and 1.46 for $T = 2$ seconds. Comparing the root loci of the system with and without the ZOH, we see that the ZOH reduces the stability margin of the discrete-data system.

In conclusion, the root loci of discrete-data systems can be constructed in the z-plane using essentially the same properties as those of the continuous-data systems in the s-plane. However, the absolute and relative stability conditions of the discrete-data system must be investigated with respect to the unit circle and the other interpretation of performance with respect to the regions in the z-plane. ◀

▶ H-9 FREQUENCY-DOMAIN ANALYSIS OF DISCRETE-DATA CONTROL SYSTEMS

All the frequency-domain methods discussed in the preceding sections can be extended to the analysis of discrete-data systems. Consider the discrete-data system shown in Fig. H-34. The closed-loop transfer function of the system is

$$\frac{Y(z)}{R(z)} = \frac{G_{ho}G(z)}{1 + G_{ho}G(z)} \tag{H-225}$$

where $G_{ho}G(z)$ is the z-transform of $G_{ho}(s)G(s)$. Just as in the case of continuous-data systems, the absolute and relative stability conditions of the closed-loop discrete-data system can be investigated by making the frequency-domain plots of $G_{ho}G(z)$. Because the positive $j\omega$-axis of the s-plane corresponds to real frequency, the frequency-domain plots of $G_{ho}G(z)$ are obtained by setting $z = e^{j\omega T}$ and then letting ω vary from 0 to ∞. This is also equivalent to mapping the points on the unit circle, $|z| = 1$, in the z-plane onto the $G_{ho}G(e^{j\omega T})$-plane. Because the unit circle repeats for every sampling frequency $\omega_s(= 2\pi/T)$, as shown in Fig. H-35, when ω is varied along the $j\omega$-axis, the frequency-domain plot of $G(e^{j\omega T})$ repeats for $\omega = n\omega_s$ to $(n + 1)\omega_s$, $n = 0, 1, 2, \ldots$. Thus, it is necessary to plot $G_{ho}G(e^{j\omega T})$ only for the range of $\omega = 0$ *to* $\omega = \omega_s$. In fact, because the unit circle in the z-plane is symmetrical about the real axis, the plot of $G_{ho}G(e^{j\omega T})$ in the polar coordinates for $\omega = 0$ to $\omega_s/2$ needs to be plotted.

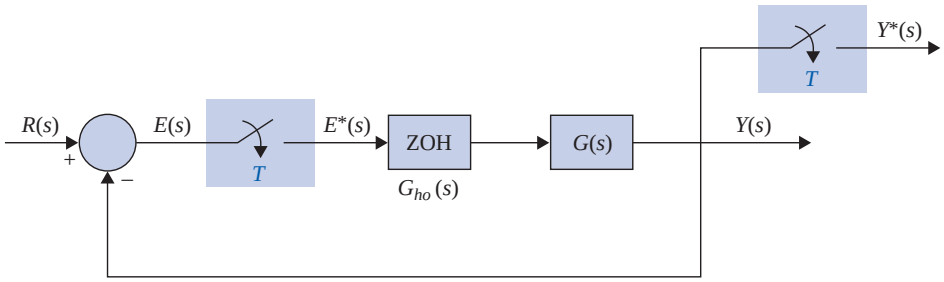

Figure H-34 Closed-loop discrete-data control system.

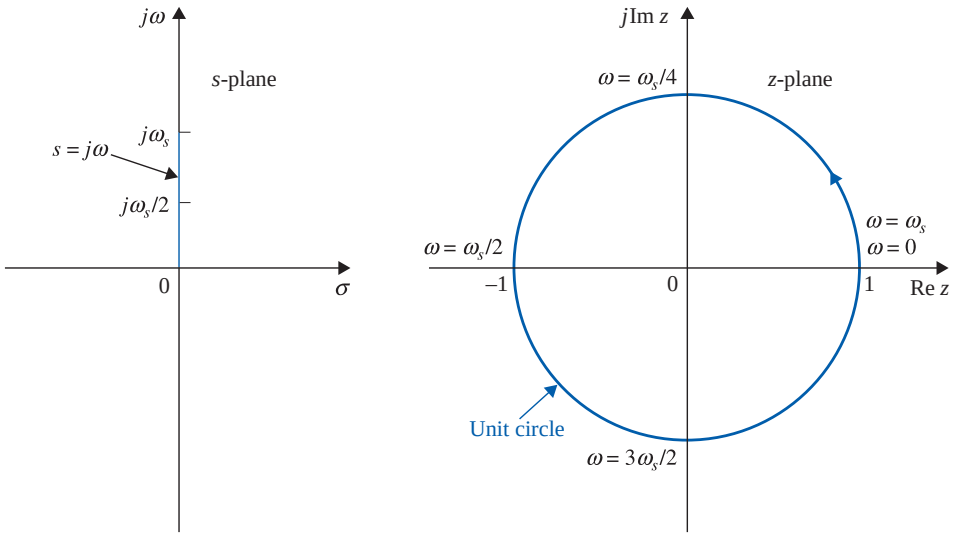

Figure H-35 Relation between the $j\omega$-axis in the s-plane and the unit circle in the z-plane.

H-9-1 Bode Plot with the *w*-Transformation

The w-transformation introduced in Eq. (H-162) can be used for frequency-domain analysis and design of discrete-data control systems. The transformation is

$$z = \frac{(2/T) + w}{(2/T) - w} \tag{H-226}$$

In the frequency domain, we set [Eq. (H-166)],

$$w = j\omega_w = j\,\frac{2}{T}\tan\frac{\omega T}{2} \tag{H-227}$$

For frequency-domain analysis of a discrete-data system, we substitute Eqs. (H-226) and (H-227) in $G(z)$ to get $G(j\omega_w)$; the latter can be used to form the Bode plot or the polar plot of the system.

▶ EXAMPLE H-9-1 As an illustrative example on frequency-domain plots of discrete-data control systems, let the transfer function of the process in the system in Fig. H-34 be

$$G(s) = \frac{1.57}{s(s+1)} \tag{H-228}$$

and the sampling frequency is 4 rad/sec. Let us first consider that the system does not have a zero-order-hold, so that

$$G_{ho}G(z) = G(z) = \frac{1.243z}{(z-1)(z-0.208)} \tag{H-229}$$

The frequency response of $G_{ho}G(z)$ is obtained by substituting $z = e^{j\omega T}$ in Eq. (H-228). The polar plot of $G_{ho}G(e^{j\omega T})$ for $\omega = 0$ *to* $\omega_s/2$ is shown in Fig. H-36. The mirror image of the locus shown, with the mirror placed on the real axis, represents the plot for $\omega = \omega_s/2$ to ω_s.

The Bode plot of $G_{ho}G(e^{j\omega T})$ consists of the graphs of $\left|G_{ho}G\left(e^{j\omega T}\right)\right|$ in dB versus ω, and $\angle G_{ho}G(e\,j\omega T)$ in degrees versus ω, as shown in Fig. H-37 for three decades of frequency with the plots ended at $\omega = \omega_s/2 = 2$ rad/sec.

For the sake of comparison, the forward-path transfer function of the system with a zero-order-hold is obtained:

$$G_{ho}G(z) = \frac{1.2215z + 0.7306}{(z-1)(z-0.208)} \tag{H-230}$$

The polar plot and the Bode plot of the last equation are shown in Figs. H-36 and H-37, respectively. Notice that the polar plot of the system with the ZOH intersects the negative real axis at a point that is closer to the $(-1, j0)$ point than that of the system without the ZOH. Thus, the system with the ZOH is less stable. Similarly, the phase of the Bode plot of the system with the ZOH is more negative than that of the system without the ZOH. The gain margin, phase margin, and peak resonance of the two systems are summarized as follows.

	Gain Margin (dB)	Phase Margin (deg)	M^r
Without ZOH	5.77	39.0	1.58
With ZOH	0.71	2.91	22.64

As an alternative, the Bode plot and polar plot of the forward-path transfer function can be done using the w-transformation of Eqs. (H-226). For the system with ZOH, the forward-path transfer function in the w-domain is

$$G_{ho}G(w) = \frac{1.57(1 + 0.504w)(1 - 1.0913w)}{w(1 + 1.197w)} \tag{H-231}$$

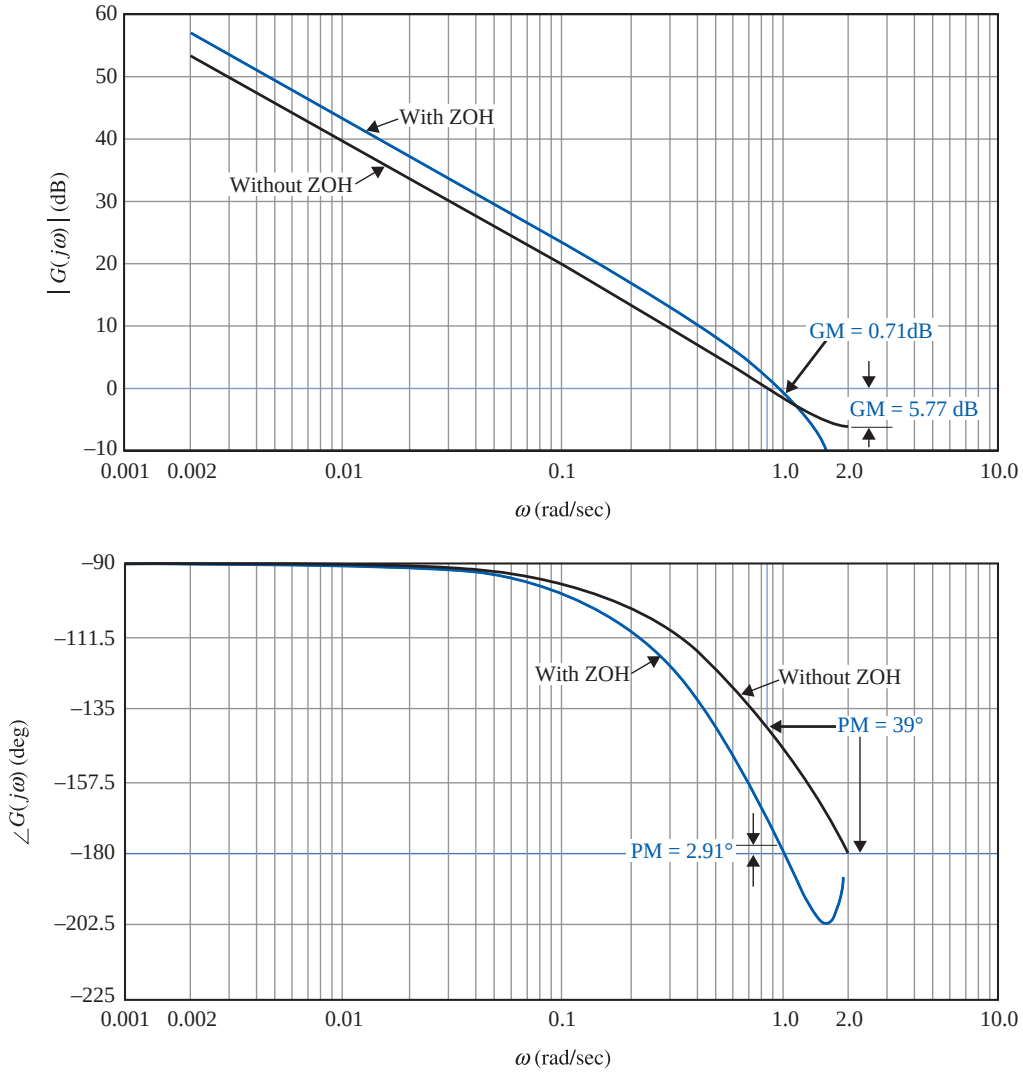

Figure H-36 Bode plot of $G_{ho}G(z)$ of the system in Fig. H-34, with $G(s) = 1.57/[s(s+1)]$. $T = 1.57$ sec, and with and without ZOH.

For the system without ZOH,

$$G_{ho}G(jw) = \frac{1 - 0.6163w^2}{w(1 + 1.978w)} \tag{H-232}$$

Substituting $w = j\omega_w$ into Eq. (H-232), the Bode plots are made as shown in Fig. H-38. Notice that the frequency coordinates in Fig. H-38 are ω_w, whereas those in Fig. H-36 are the real frequency ω. The two frequencies are related through Eq. (H-227).

The conclusion from this illustrative example is that, once z is replaced by $e^{j\omega T}$ in the z-domain transfer function, or if the w-transform is used, all the frequency-domain analysis techniques available for continuous-data systems can be applied to discrete-data systems. ◀

▶ H-10 DESIGN OF DISCRETE-DATA CONTROL SYSTEMS

H-10-1 Introduction

The design of discrete-data control systems is similar in principle to the design of continuous-data control systems. The design objective is basically that of determining the controller so that the system will perform in accordance with specifications. In fact, in

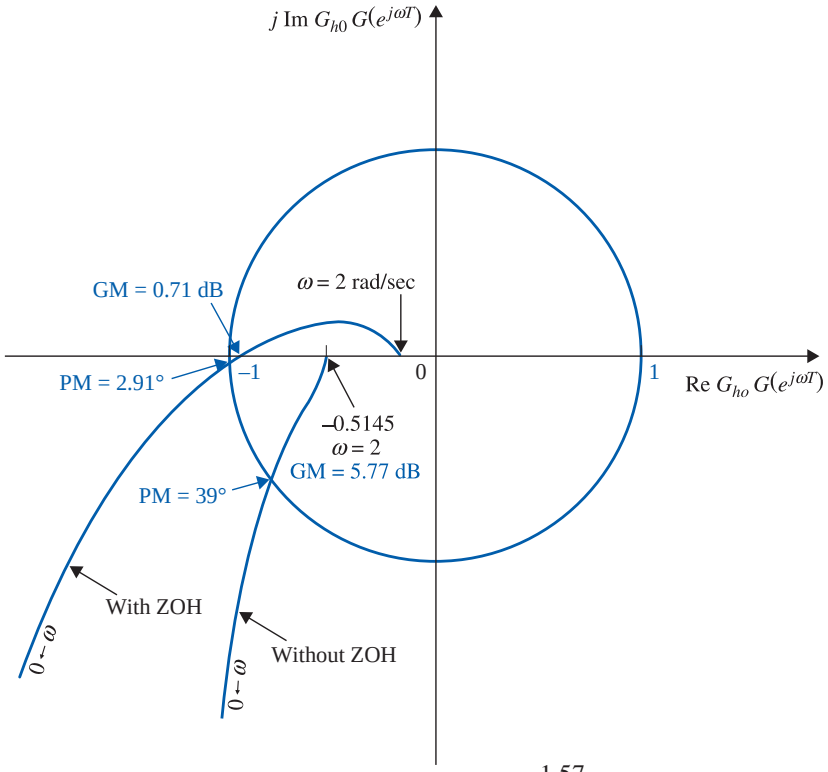

Figure H-37 Frequency-domain plot of $G(s) = \dfrac{1.57}{s(s+1)}$, $T = 1.57$ seconds, and with and without ZOH.

most situations, the controlled process is the same, except in discrete-data systems the controller is designed to process sampled or digital data.

The design of discrete-data control systems treated in this chapter is intended only for introductory purposes. An in-depth coverage of the subject may be found in books dedicated to digital control. In this chapter we deal only with the design of a control system with a cascade digital controller and a system with digital state feedback. Block diagrams of these systems are shown in Fig. H-39.

Just as with the design of continuous-data control systems, the design of discrete-data control systems can be carried out in either the frequency domain or the time domain. Using computer programs, digital control systems can be designed with a minimum amount of trial and error.

H-10-2 Digital Implementation of Analog Controllers

It seems that most people learn how to design continuous-data systems before they learn to design digital systems, if at all. Therefore, it is not surprising that most engineers prefer to design continuous-data systems. Ideally, if the designer intends to use digital control, the system should be designed so that the dynamics of the controller can be described by a z-transfer function or difference equations. However, there are situations in which the analog controller is already designed, but the availability and advantages of digital control suggest that the controller be implemented by digital elements. Thus, the

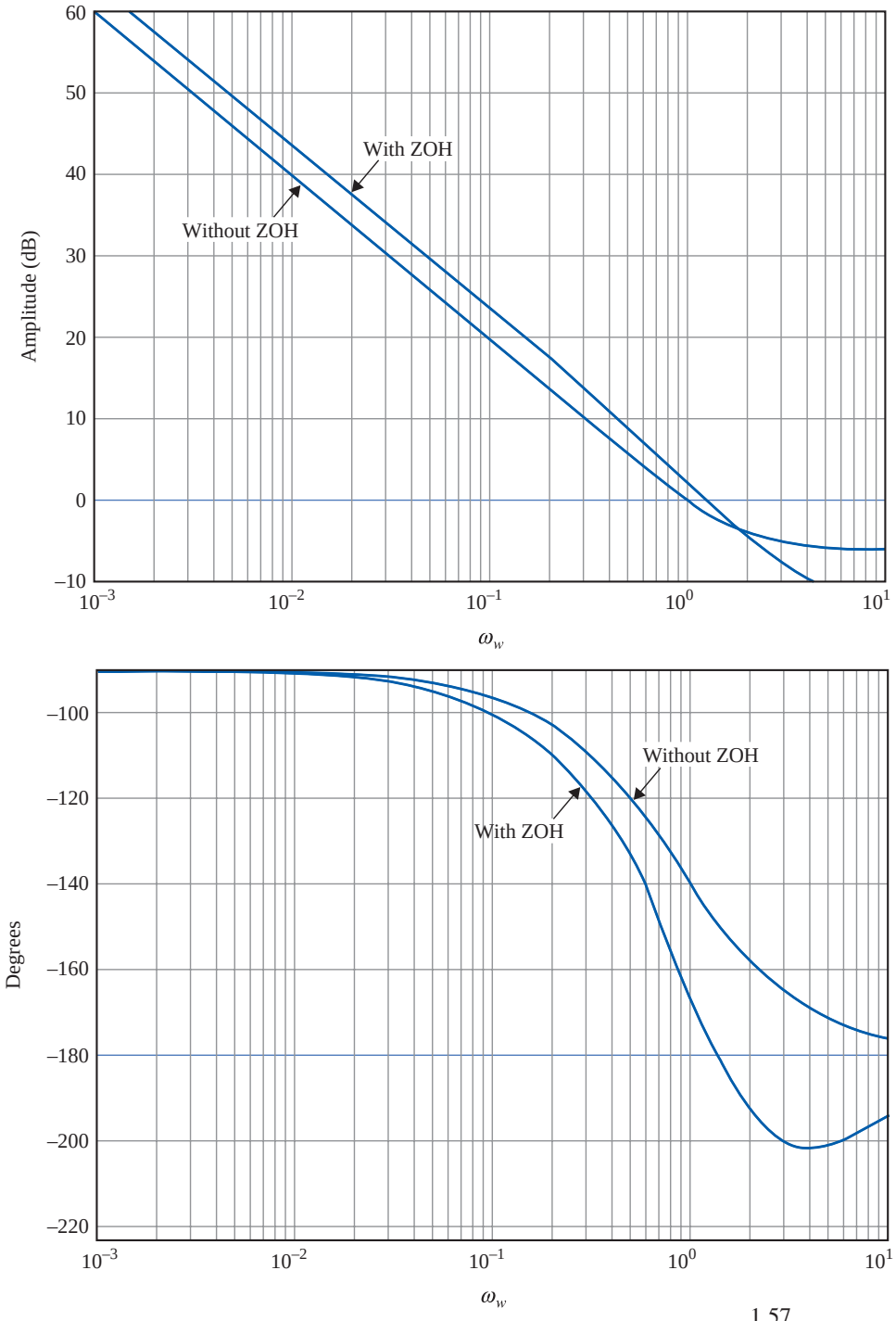

Figure H-38 Bode plot of $G_{ho}G(z)$ of the system in Fig. H-34 with $G(s) = \dfrac{1.57}{s(s+1)}$, $T = 1.57$ seconds, with and without ZOH. The plots are done with the w-transformation, $w = j\omega_w$.

problems discussed in this section are twofold: first how continuous-data controllers such as PID, phase-lead or phase-lag controllers, and others can be approximated by digital controllers and, second, the problem of implementing digital controllers by digital processors.

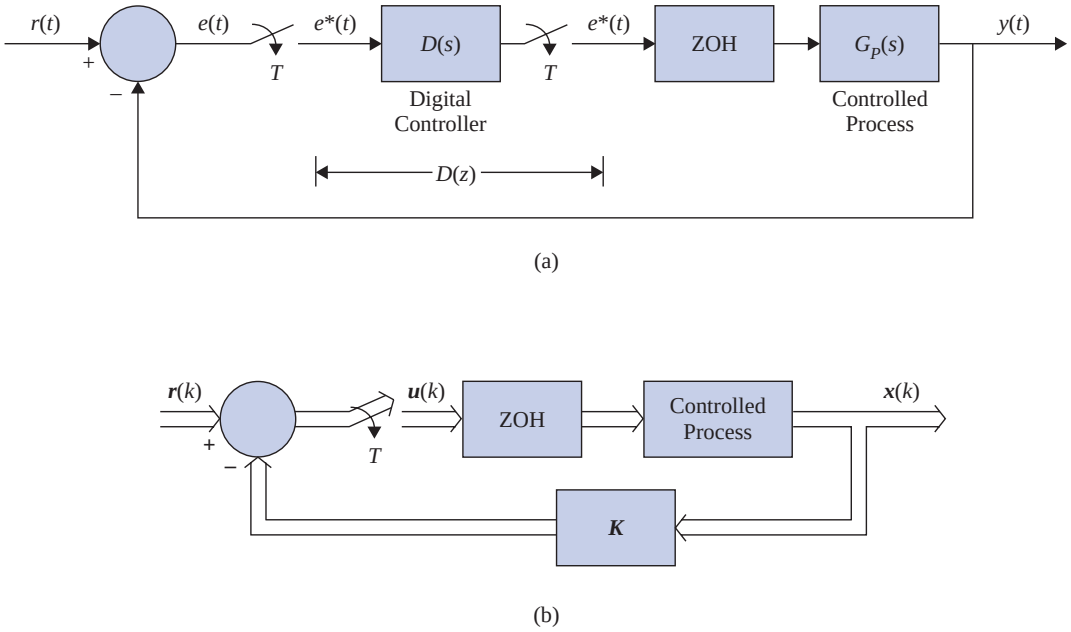

Figure H-39 (a) Digital control system with cascade digital controller. (b) Digital control system with state feedback.

H-10-3 Digital Implementation of the PID Controller

The PID controller in the continuous-data domain is described by

$$G_c(s) = K_P + K_D s + \frac{K_I}{s} \tag{H-233}$$

The proportional component K_P is implemented digitally by a constant gain K_P. Because a digital computer or processor has finite word length, the constant K_P cannot be realized with infinite resolution.

The time derivative of a function $f(t)$ at $t = kT$ can be approximated by the **backward-difference rule**, using the values of $f(t)$ measured at $t = kT$ and $(k - 1)\,T$; that is,

$$\left.\frac{df(t)}{dt}\right|_{t=kT} = \frac{1}{T}\,(\,f(kT) - f[(k-1)T]) \tag{H-234}$$

To find the z-transfer function of the derivative operation described before, we take the z-transform on both sides of Eq. (H-234). We have

$$\mathcal{Z}\left(\left.\frac{df(t)}{dt}\right|_{t=kT}\right) = \frac{1}{T}\left(1 - z^{-1}\right)F(z) = \frac{z-1}{Tz}F(z) \tag{H-235}$$

Thus, the z-transfer function of the digital differentiator is

$$G_D(z) = K_D\,\frac{z-1}{Tz} \tag{H-236}$$

where K_D is the proportional constant of the derivative controller. Replacing z by e^{Ts} in Eq. (H-236), we can show that, as the sampling period T approaches zero, $G_D(z)$ approaches $K_D s$, which is the transfer function of the analog derivative controller. In general, the choice of the sampling period is extremely important. The value of T should be sufficiently small so that the digital approximation is adequately accurate.

There are a number of numerical integration rules that can be used to digitally approximate the integral controller K_I/s. The three basic methods of approximating the area of a function numerically are **trapezoidal integration**, **forward-rectangular integration**, and **backward-rectangular integration**. These are described as follows.

Trapezoidal Integration

The trapezoidal-integration rule approximates the area under the function $f(t)$ by a series of trapezoids, as shown in Fig. H-40. Let the integral of $f(t)$ evaluated at $t = kT$ be designated as $u(kT)$. Then,

$$u(kT) = u[(k-1)T] + \frac{T}{2}\{f(kT) - f[(k-1)T]\} \tag{H-237}$$

where the area under $f(t)$ for $(k-1)T \leq t < kT$ is approximated by the area of the trapezoid in the interval. Taking the z-transform on both sides of Eq. (H-237), we have the transfer function of the digital integrator as

$$G_I(z) = K_I \frac{U(z)}{F(z)} = \frac{K_I T(z+1)}{2(z-1)} \tag{H-238}$$

where K_I is the proportional constant.

Forward-Rectangular Integration

For the forward-rectangular integration, we approximate the area under $f(t)$ by rectangles, as shown in Fig. H-41. The integral of $f(t)$ at $t = kT$ is approximated by

$$u(kT) = u[(k-1)T] + Tf(kT) \tag{H-239}$$

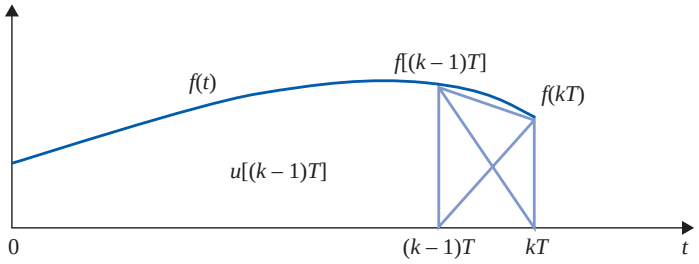

Figure H-40 Trapezoidal-integration rule.

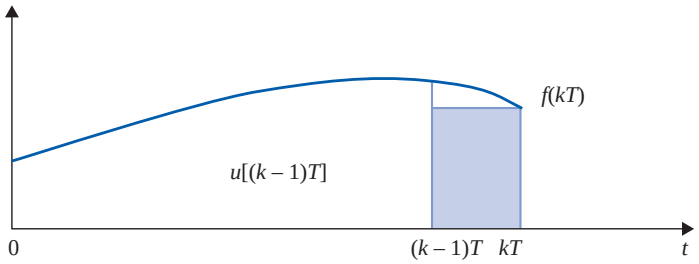

Figure H-41 Forward-rectangular integration rule.

By taking the z-transform on both sides of Eq. (H-239), the transfer function of the digital integrator using the forward-rectangular rule is

$$G_I(z) = K_I \frac{U(z)}{F(z)} = \frac{K_I T z}{z-1} \tag{H-240}$$

Backward-Rectangular Integration

For the backward-rectangular integration, the digital approximation rule is illustrated in Fig. H-42. The integral of $f(t)$ at $t = kT$ is approximated by

$$u(kT) = u[(k-1)T] + Tf[(k-1)T] \tag{H-241}$$

The z-transfer function of the digital integrator using the backward-rectangular integration rule is

$$G_I(z) = K_I \frac{U(z)}{F(z)} = \frac{K_I T}{z-1} \tag{H-242}$$

By combining the proportional, derivative, and integration operations described previously, the digital PID controller is modeled by the following transfer functions.

Trapezoidal Integration

$$G_c(z) = \frac{\left(K_P + \frac{TK_I}{2} + \frac{K_D}{T}\right)z^2 + \left(\frac{TK_I}{2} - K_P - \frac{2K_D}{T}\right)z + \frac{K_D}{T}}{z(z-1)} \tag{H-243}$$

Forward-Rectangular Integration

$$G_c(z) = \frac{\left(K_P + \frac{K_D}{T} + TK_I\right)z^2 - \left(K_P + \frac{2K_D}{T}\right)z + \frac{K_D}{T}}{z(z-1)} \tag{H-244}$$

Backward-Rectangular Integration

$$G_c(z) = \frac{\left(K_P + \frac{K_D}{T}\right)z^2 + \left(TK_I - K_P - \frac{2K_D}{T}\right)z + \frac{K_D}{T}}{z(z-1)} \tag{H-245}$$

When $K_I = 0$, the transfer function of the digital PD controller is

$$G_c(z) = \frac{\left(K_P + \frac{K_D}{T}\right)z - \frac{K_D}{T}}{z} \tag{H-246}$$

Once the transfer function of a digital controller is determined, the controller can be implemented by a digital processor or computer. The operator z^{-1} is interpreted as a time delay of T seconds. In practice, the time delay is implemented by storing a variable in some

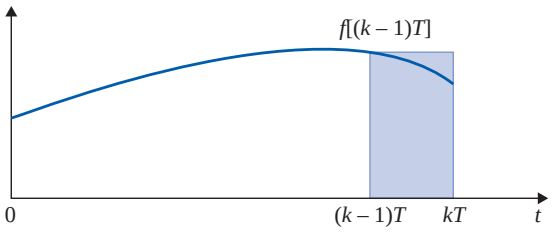

Figure H-42 Backward-rectangular integration rule.

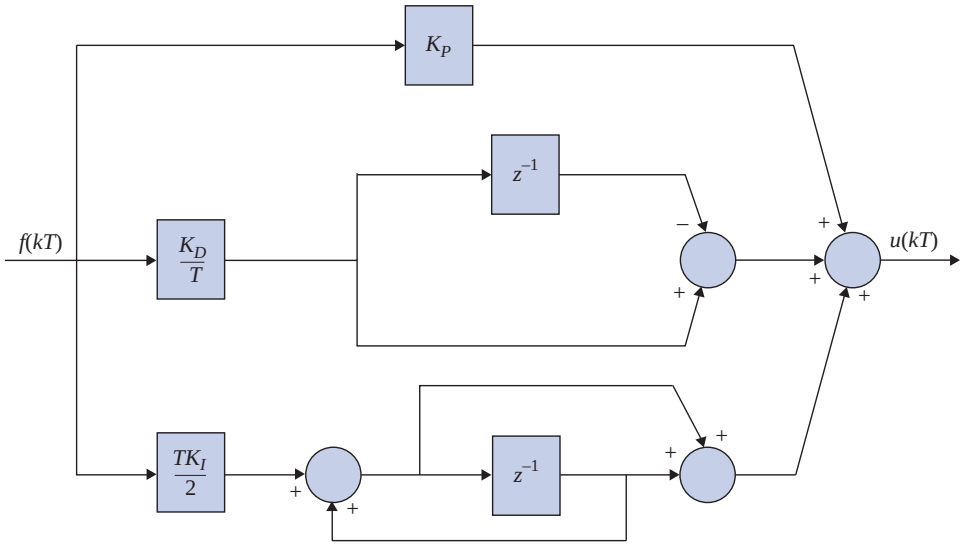

Figure H-43 Block diagram of a digital-program implementation of the PID controller.

storage location in the computer and then taking it out after T seconds have elapsed. Fig. H-43 illustrates a block diagram representation of the digital program of the PID controller using the trapezoidal-integration rule.

H-10-4 Digital Implementation of Lead and Lag Controllers

In principle, any continuous-data controller can be made into a digital controller simply by adding sample-and-hold units at the input and the output terminals of the controller and selecting a sampling frequency as small as is practical. Figure H-44 illustrates the basic scheme with $G_c(s)$, the transfer function of the continuous-data controller, and $G_c(z)$, the equivalent digital controller. The sampling period T should be sufficiently small so that the dynamic characteristics of the continuous-data controller are not lost through the digitization. The system configuration in Fig. H-44 actually suggests that, given the continuous-data controller $G_c(s)$, the equivalent digital controller $G_c(z)$ can be obtained by the arrangement shown. On the other hand, given the digital controller $G_c(z)$, we can realize it by using an analog controller $G_c(s)$ and sample-and-hold units, as shown in Fig. H-44.

▶ **EXAMPLE H-10-1** As an illustrative example, consider that the continuous-data controller in Fig. H-44 is represented by the transfer function

$$G_c(s) = \frac{s+1}{s+1.61} \tag{H-247}$$

From Fig. H-44, the transfer function of the digital controller is written

$$G_c(z) = \frac{U(z)}{F(z)} = (1 - z^{-1})\mathcal{Z}\left[\frac{s+1}{s(s+1.61)}\right] = \frac{z - (0.62e^{-1.61T} + 0.38)}{z - e^{-1.61T}} \tag{H-248}$$

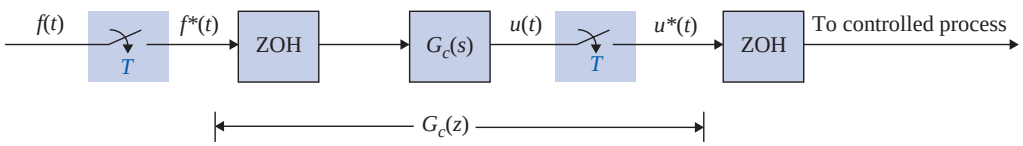

Figure H-44 Realization of a digital controller by an analog controller with sample-and-hold units.

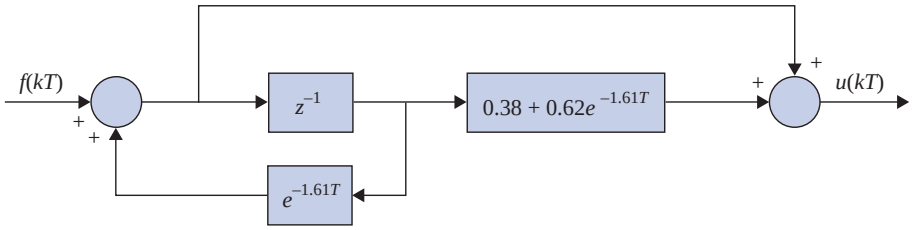

Figure H-45 Digital-program realization of Eq. (H-248).

The digital-program implementation of Eq. (H-248) is shown in Fig. H-45. ◀

▶ H-11 DIGITAL CONTROLLERS

Digital controllers can be realized by digital networks, digital computers, microprocessors, or digital signal processors (DSPs). A distinct advantage of digital controllers implemented by microprocessors or DSPs is that the control algorithm contained in the controller can be easily altered by changing the program. Changing the components of a continuous-data controller is rather difficult once the controller has been built.

H-11-1 Physical Realizability of Digital Controllers

The transfer function of a digital controller can be expressed as

$$G_c(z) = \frac{E_2(z)}{E_1(z)} = \frac{b_0 + b_1 z^{-1} + \cdots + b_m z^{-m}}{a_0 + a_1 z^{-1} + \cdots + a_n z^{-n}} \tag{H-249}$$

where n and m are positive integers. The transfer function $G_c(z)$ is said to be physically realizable if its output does not precede any input. This means that the series expansion of $G_c(z)$ should not have any positive powers in z. In terms of the $G_c(z)$ given in Eq. (H-249), if $b_0 \neq 0$, then $a_0 \neq 0$. If $G_c(z)$ is expressed as

$$G_c(z) = \frac{b_m z^m + b_{m-1} z^{m-1} + \cdots + b_1 z + b_0}{a_n z^n + a_{n-1} z^{n-1} + \cdots + a_1 z + a_0} \tag{H-250}$$

then the physical realizability requirement is $n \geq m$.

The decomposition techniques presented in Chapter 2 can be applied to realize the digital controller transfer function by a digital program. We consider that a digital program is capable of performing arithmetic operations of addition, subtraction, multiplication by a constant, and shifting. The three basic methods of decomposition for digital programming are discussed in the following sections.

Digital Program by Direct Decomposition

Applying direct decomposition to Eq. (H-249), we have the following equations:

$$E_2(z) = \frac{1}{a_0}\left(b_0 + b_1 z^{-1} + \cdots + b_m z^{-m}\right) X(z) \tag{H-251}$$

$$X(z) = \frac{1}{a_0} E_1(z) - \frac{1}{a_0}\left(a_1 z^{-1} + a_2 z^{-2} + \cdots + a_n z^{-n}\right) X(z) \tag{H-252}$$

Fig. H-46 shows the signal-flow graph of a direct digital program of Eq. (H-249) by direct decomposition for $m = 2$ and $n = 3$. The branches with gains of z^{-1} represent time delays or shifts of one sampling period.

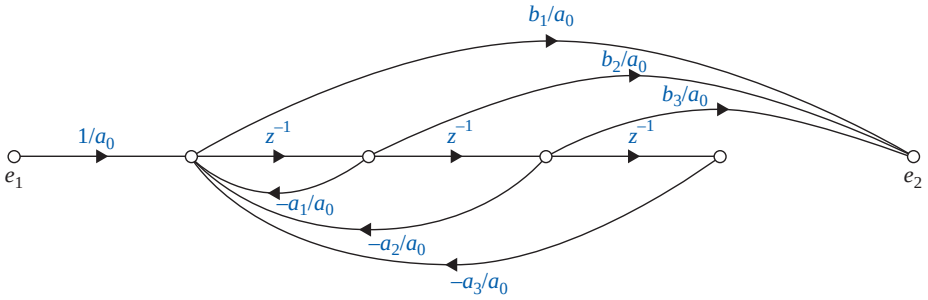

Figure H-46 Signal-flow graph of digital program by direct decomposition of Eq. (H-249) with $n = 3$ and $m = 2$.

Digital Program by Cascade Decomposition

The transfer function $G_c(z)$ can be written as a product of first- or second-order transfer functions, each realizable by a simple digital program. The digital program of the overall transfer function is then represented by these simple digital programs connected in cascade. Eq. (H-249) is written in factored form as

$$G_c(z) = G_{c1}(z)G_{c2}(z)\cdots G_{cn}(z) \tag{H-253}$$

where the individual factors can be expressed as

Real Pole and Zero

$$G_{ci}(z) = K_i \frac{1 + c_i z^{-1}}{1 + d_i z^{-1}} \tag{H-254}$$

Complex-Conjugate Poles (No Zeros)

$$G_{ci}(z) = \frac{K_i}{1 + d_{i1} z^{-1} + d_{i2} z^{-2}} \tag{H-255}$$

Complex-Conjugate Poles with One Zero

$$G_{ci}(z) = K_i \frac{1 + c_i z^{-1}}{1 + d_{i1} z^{-1} + d_{i2} z^{-2}} \tag{H-256}$$

and several other possible forms up to the second order.

Digital Program by Parallel Decomposition

The transfer function in Eq. (H-249) can be expanded into a sum of simple first- or second-order terms by partial-fraction expansion. These terms are then realized by digital programs connected in parallel.

▶ **EXAMPLE H-11-1** Consider the following transfer function of a digital controller:

$$G_c(z) = \frac{E_2(z)}{E_1(z)} = \frac{10\left(1 + 0.5z^{-1}\right)}{(1 - z^{-1})(1 - 0.2z^{-1})} \tag{H-257}$$

Because the leading coefficients of the numerator and denominator polynomials in z^{-1} are all constants, the transfer function is physically realizable. The transfer function $G_c(z)$ is realized by the three types of digital programs discussed earlier. ◀

Direct Digital Programming

Eq. (H-257) is written

$$G_c(z) = \frac{E_2(z)}{E_1(z)} = \frac{10(1 + 0.5z^{-1})X(z)}{(1 - z^{-1})(1 - 0.2z^{-1})X(z)} \tag{H-258}$$

Expanding the numerator and denominator of the last equation and equating, we have

$$E_2(z) = (10 + 5z^{-1})X(z) \tag{H-259}$$

$$X(z) = E_1(z) + 1.2z^{-1}X(z) - 0.2z^{-2}X(z) \tag{H-260}$$

The last two equations are realized by the digital program shown in Fig. H-47.

Cascade Digital Programming

The right-hand side of Eq. (H-257) is divided into two factors in one of several possible ways.

$$G_c(z) = \frac{E_2(z)}{E_1(z)} = \frac{1 + 0.5z^{-1}}{1 - z^{-1}} \frac{10}{1 - 0.2z^{-1}} \tag{H-261}$$

Fig. H-48 shows the signal-flow graph of the cascade digital program of the controller.

Parallel Digital Programming

The right-hand side of Eq. (H-257) is expanded by partial fraction into two separate terms.

$$G_c(z) = \frac{E_2(z)}{E_1(z)} = \frac{18.75}{1 - z^{-1}} - \frac{8.75}{1 - 0.2z^{-1}} \tag{H-262}$$

Fig. H-49 shows the signal-flow graph of the parallel digital program of the controller.

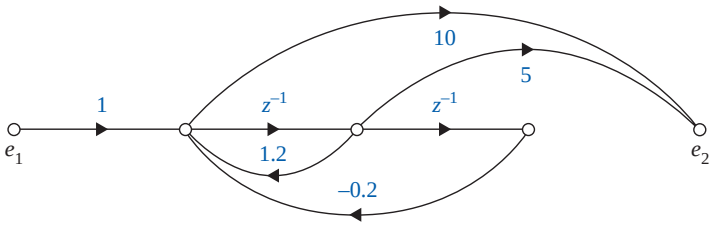

Figure H-47 Direct digital program of Eq. (H-257).

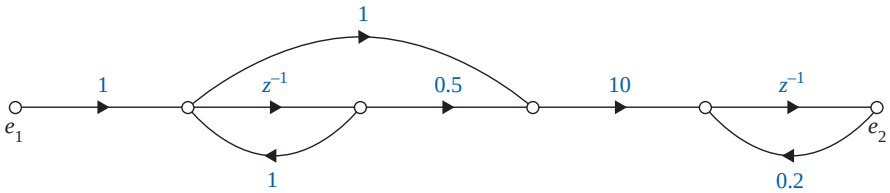

Figure H-48 Cascade digital program of Eq. (H-257).

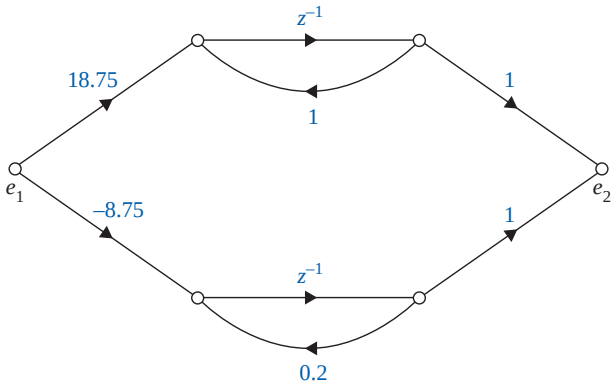

Figure H-49 Parallel digital program of Eq. (H-257).

▶ H-12 DESIGN OF DISCRETE-DATA CONTROL SYSTEMS IN THE FREQUENCY DOMAIN AND THE *z*-PLANE

The *w*-transformation introduced in Section H-5 can be used to carry out the design of discrete-data control systems in the frequency domain. Once the transfer function of the controlled process is transformed into the *w*-domain, all the design techniques for continuous-data control systems can be applied to the design of discrete-data systems.

H-12-1 Phase-Lead and Phase-Lag Controllers in the *w*-Domain

Just as in the *s*-domain, the single-stage phase-lead and phase-lag controllers in the *w*-domain can be expressed by the transfer function

$$G_c(w) = \frac{1 + a\tau w}{1 + \tau w} \tag{H-263}$$

where $a > 1$ corresponds to phase lead and $a < 1$ corresponds to phase lag. When w is replaced by $j\omega_w$, the Bode plots of Eq. (H-263) are identical to those of Figs. 9-28 and 9-45 for $a > 1$ and $a < 1$, respectively. Once the controller is designed in the *w*-domain, the *z*-domain controller is obtained by substituting the *w*-transformation relationship in Eq. (H-163); that is,

$$w = \frac{2}{T}\frac{z - 1}{z + 1} \tag{H-264}$$

The following example illustrates the design of a discrete-data control system using the *w*-transformation in the frequency domain and the *z*-plane.

▶ EXAMPLE H-12-1 Consider the sun-seeker control system described in Section 4-11 and shown in Fig. 9-29. Now let us assume that the system has discrete data so that there is a ZOH in the forward path. The sampling period is 0.01 second. The transfer function of the controlled process is

$$G_p(s) = \frac{2500}{s(s + 25)} \tag{H-265}$$

The *z*-transfer function of the forward path, including the sample-and-hold, is

$$G_{h0}G_p(z) = (1 - z^{-1})\mathcal{Z}\left(\frac{2500}{s^2(s + 25)}\right) \tag{H-266}$$

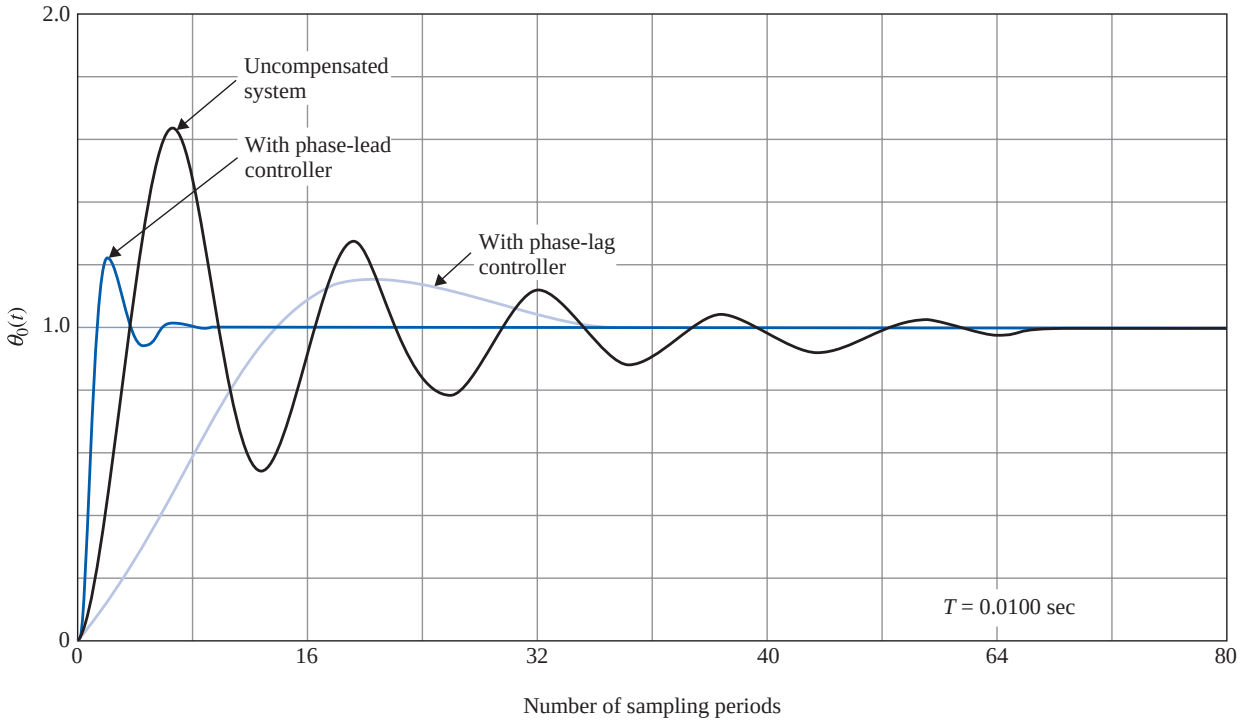

Figure H-50 Step responses of discrete-data sun-seeker system in Example H-12-1.

Carrying out the z-transform in the last equation with $T = 0.01$ second, we get

$$G_{h0}G_p(z) = \frac{0.1152z + 0.106}{(z-1)(z-0.7788)} \tag{H-267}$$

The closed-loop transfer function of the discrete-data system is

$$\frac{\Theta_o(z)}{\Theta_r(z)} = \frac{G_{h0}G_p(z)}{1 + G_{h0}G_p(z)} = \frac{0.1152z + 0.106}{z^2 - 1.6636z + 0.8848} \tag{H-268}$$

The unit-step response of the uncompensated system is shown in Fig. H-50. The maximum overshoot is 66%.

Let us carry out the design in the frequency domain using the w-transformation of Eq. (H-162),

$$z = \frac{(2/T) + w}{(2/T) - w} \tag{H-269}$$

Substituting Eq. (H-269) into Eq. (H-268), we have

$$G_{h0}G_p(w) = \frac{100(1 - 0.005w)(1 + 0.000208w)}{w(1 + 0.0402w)} \tag{H-270}$$

The Bode plot of the last equation is shown in Fig. H-51. The gain and phase margins of the uncompensated system are 6.39 dB and 14.77°, respectively.

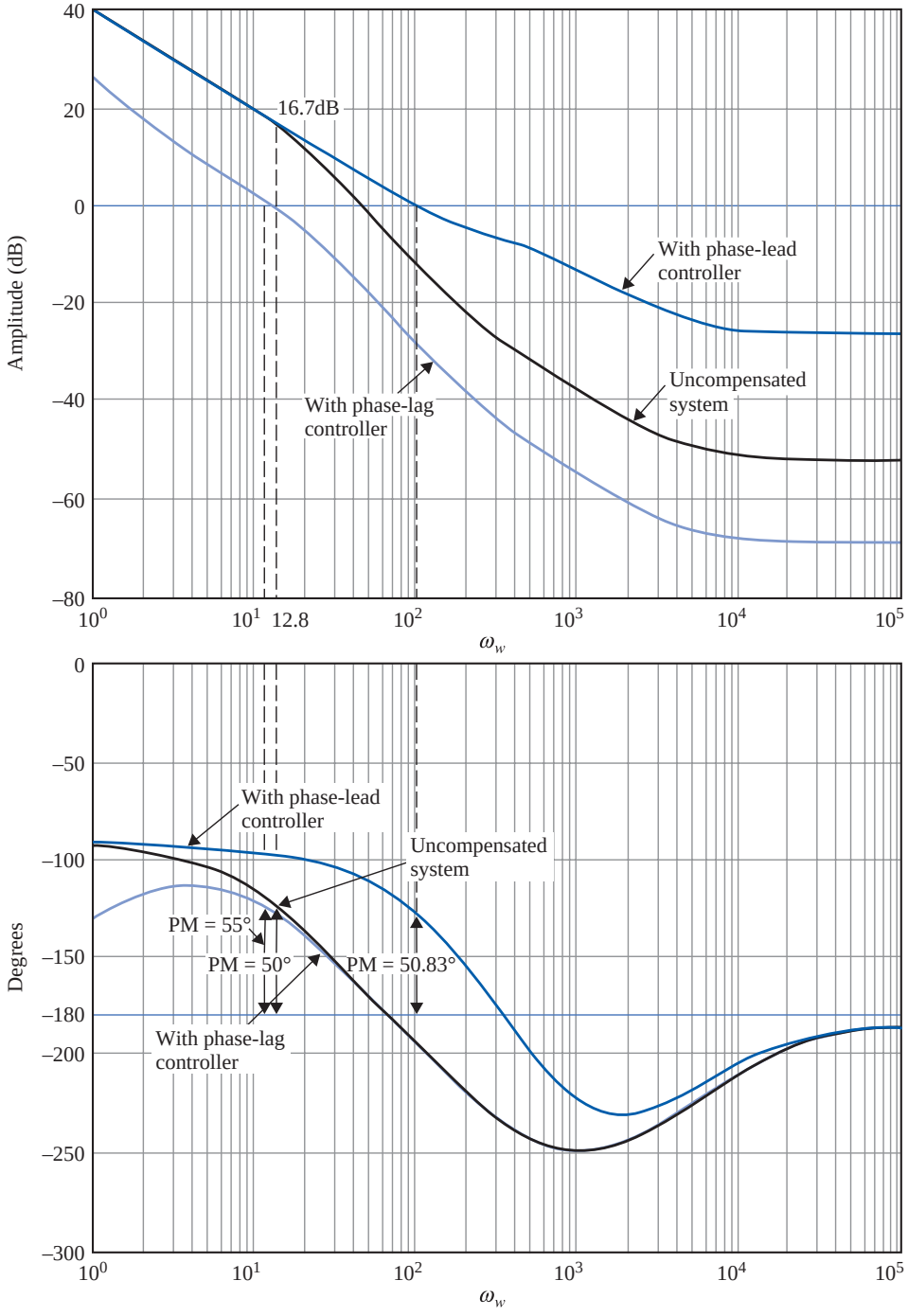

Figure H-51 Bode plots of discrete-data sun-seeker system in Example H-12-1.

Phase-Lag Controller Design in the Frequency Domain

Let us first design the system using a phase-lag controller with the transfer function given in Eq. (H-263) with $a < 1$. Let us require that the phase margin of the system be at least 50°.

From the Bode plot in Fig. H-51, a phase margin of 50° can be realized if the gain crossover point is at $\omega_w = 12.8$ and the gain of the magnitude curve of $G_{ho}G_p(j\omega_w)$ is 16.7 dB.

Thus, we need -16.7 dB of attenuation to bring the magnitude curve down so that it will cross the 0-dB-axis at $\omega_w = 12.8$. We set

$$20 \log_{10} a = -16.7 \text{ dB} \tag{H-271}$$

from which we get $a = 0.1462$. Next, we set $1/a\tau$ to be at least one decade below the gain-crossover point at $\omega_w = 12.8$. We set

$$\frac{1}{a\tau} = 1 \tag{H-272}$$

Thus,

$$\frac{1}{\tau} = a = 0.1462 \tag{H-273}$$

The phase-lag controller in the w-domain is

$$G_c(w) = \frac{1 + a\tau w}{1 + \tau w} = \frac{1 + w}{1 + 6.84w} \tag{H-274}$$

Substituting the z-w-transform relation, $w = (2/T)(z - 1)/(z + 1)$, in Eq. (H-274), the phase-lag controller in the z-domain is obtained:

$$G_c(z) = 0.1468 \frac{z - 0.99}{z - 0.9985} \tag{H-275}$$

The Bode plot of the forward-path transfer function with the phase-lag controller of Eq. (H-274) is shown in Fig. H-51. The phase margin of the compensated system is improved to 55°. The unit-step response of the phase-lag compensated system is shown in Fig. H-50. The maximum overshoot is reduced to 16%.

Phase-Lead Controller Design in the Frequency Domain

A phase-lead controller is obtained by using $a > 1$ in Eq. (H-263). The same principle for the design of phase-lead controllers of continuous-data systems described in Chapter 9 can be applied here. Because the slope of the phase curve near the gain crossover is rather steep, as shown in Fig. H-51, it is expected that some difficulty may be encountered in designing a phase-lead controller for the system. Nevertheless, we can assign a relatively large value for a, rather than using the amount of phase lead required as a guideline.

Let us set $a = 20$. The gain of the controller at high values of ω_w is

$$20 \log_{10} a = 20 \log_{10} 20 = 26 \text{ dB} \tag{H-276}$$

From the design technique outlined in Chapter 9, the new gain crossover should be located at the point where the magnitude curve is at $-26/2 = -13$ dB. Thus, the geometric mean of the two corner frequencies of the phase-lead controller should be at the point where the magnitude of $G_{ho}G_p(j\omega)$ is -13 dB. From Fig. H-51 this is found to be at $\omega_w = 115$. Thus,

$$\frac{1}{\tau} = 115\sqrt{a} = 514 \tag{H-277}$$

The w-domain transfer function of the phase-lead controller is

$$G_c(w) = \frac{1 + a\tau w}{1 + \tau w} = \frac{1 + 0.03888w}{1 + 0.001944w} \tag{H-278}$$

The transfer function of the phase-lead controller in the z-domain is

$$G_c(z) = \frac{8.7776z - 6.7776}{1.3888z + 0.6112} \tag{H-279}$$

The Bode plot of the phase-lead compensated system is shown in Fig. H-51. The phase margin of the compensated system is 50.83°. The unit-step response of the phase-lead compensated system is shown in Fig. H-50. The maximum overshoot is 27%, but the rise time is faster.

Digital PD-Controller Design in the *z*-Plane

The digital PD controller is described by the transfer function in Eq. (H-246) and is repeated as

$$G_c(z) = \frac{\left(K_P + \dfrac{K_D}{T}\right)z - \dfrac{K_D}{T}}{z} \tag{H-280}$$

To satisfy the condition that $G_c(1) = 1$ so that $G_c(z)$ does not affect the steady-state error of the system, we set $K_P = 1$. Applying the digital PD controller as a cascade controller to the sun-seeker system, the forward-path transfer function of the compensated system is

$$G_c(z)G_{ho}G_p(z) = \frac{(1 + 100K_D)z - 100K_D}{z} \frac{0.1152z + 0.106}{(z - 1)(z - 0.7788)} \tag{H-281}$$

We can use the root-contour method to investigate the effects of varying K_D. The characteristic equation of the closed-loop system is

$$z(z^2 - 1.6636z + 0.8848) + 11.52K_D(z - 1)(z + 0.9217) = 0 \tag{H-282}$$

Dividing both sides of the last equation by the terms that do not contain K_D, the equivalent forward-path transfer function with K_D appearing as a multiplying factor is

$$G_{eq}(z) = \frac{11.52K_D(z - 1)(z + 0.9217)}{z(z^2 - 1.6636z + 0.8848)} \tag{H-283}$$

The root contours of the system for $K_D > 0$ are shown in Fig. H-52. These root contours show that the effectiveness of the digital PD controller is limited for this system, since the contours do not dip low enough toward the real axis. In fact, we can show that the best value of K_D from the standpoint of overshoot is 0.022, and the maximum overshoot is 28%.

Digital PE-Controller Design in the *z*-Plane

The digital PI controller introduced in Section H-10-3 can be used to improve the steady-state performance by increasing the system type and, at the same time, improve the relative stability by using the *dipole* principle. Let us select the backward-rectangular integration implementation of the PID controller given by Eq. (H-245). With $K_D = 0$, the transfer function of the digital PI controller becomes

$$G_c(z) = \frac{K_P z - (K_P - K_I T)}{z - 1} = K_P \frac{z - \left(1 - \dfrac{K_I T}{K_P}\right)}{z - 1} \tag{H-284}$$

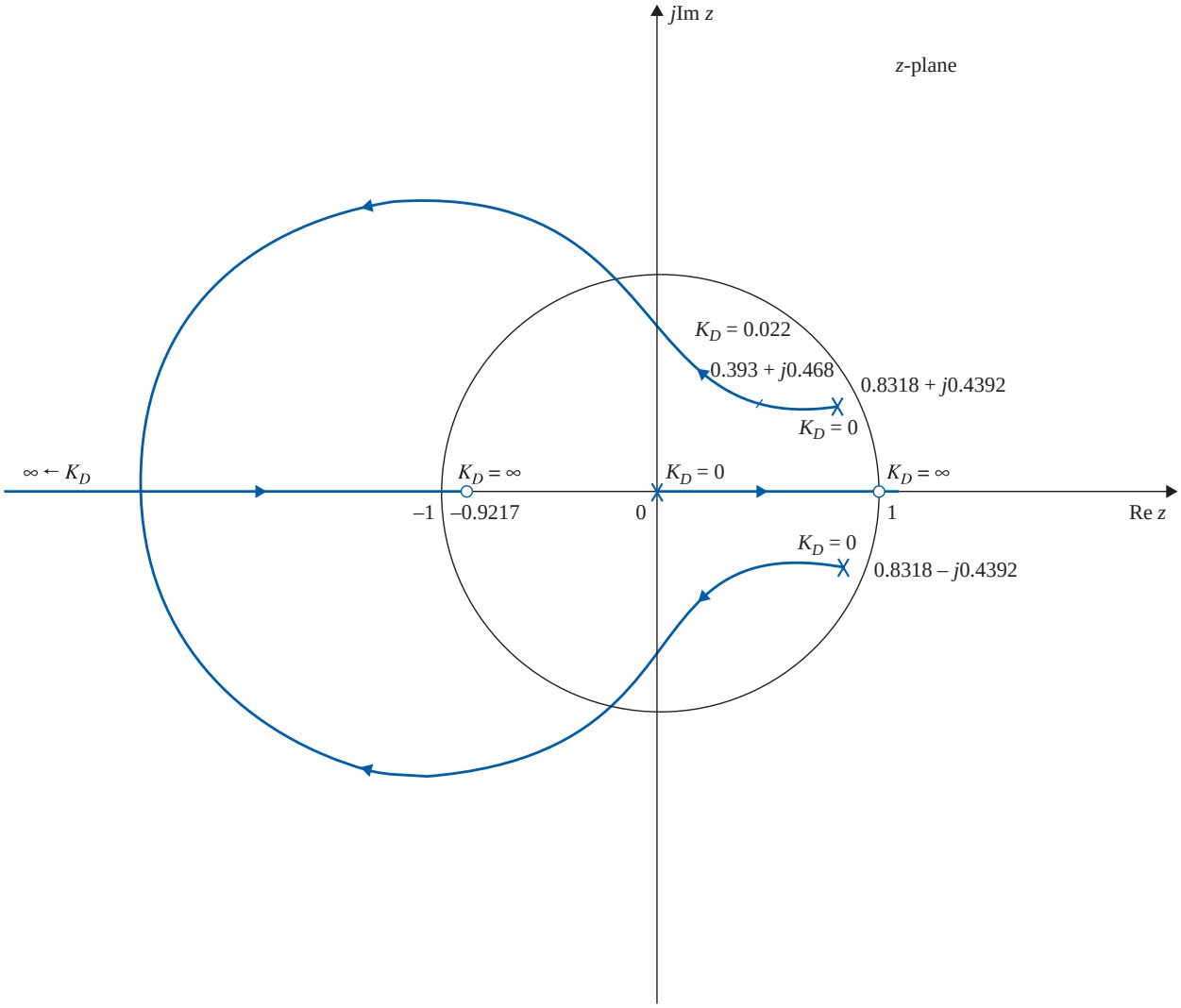

Figure H-52 Root contours of sun-seeker system in Example H-12-1 with digital PD controller. K_D varies.

The principle of the dipole design of the PI controller is to place the zero of $G_c(z)$ very close to the pole at $z = 1$. The effective gain provided by the controller is essentially equal to K_P.

To create a root-locus problem, the transfer function in Eq. (H-267) is written

$$G_{ho}G_p(z) = \frac{K(z + 0.9217)}{(z - 1)(z - 0.7788)} \tag{H-285}$$

where $K = 0.1152$. The root loci of the system are drawn as shown in Fig. H-53. The roots of the characteristic equation when $K = 0.1152$ are $0.8318 + j0.4392$ and $0.8318 - j0.4392$. As shown earlier, the maximum overshoot of the system is 66%. If K is reduced to 0.01152, the characteristic equation roots are at $0.8836 + j0.0926$ and $0.8836 - j0.0926$. The maximum overshoot is reduced to only 3%.

We can show that, if the gain in the numerator of Eq. (H-265) is reduced to 250, the maximum overshoot of the system would be reduced to 3%. This means to realize a

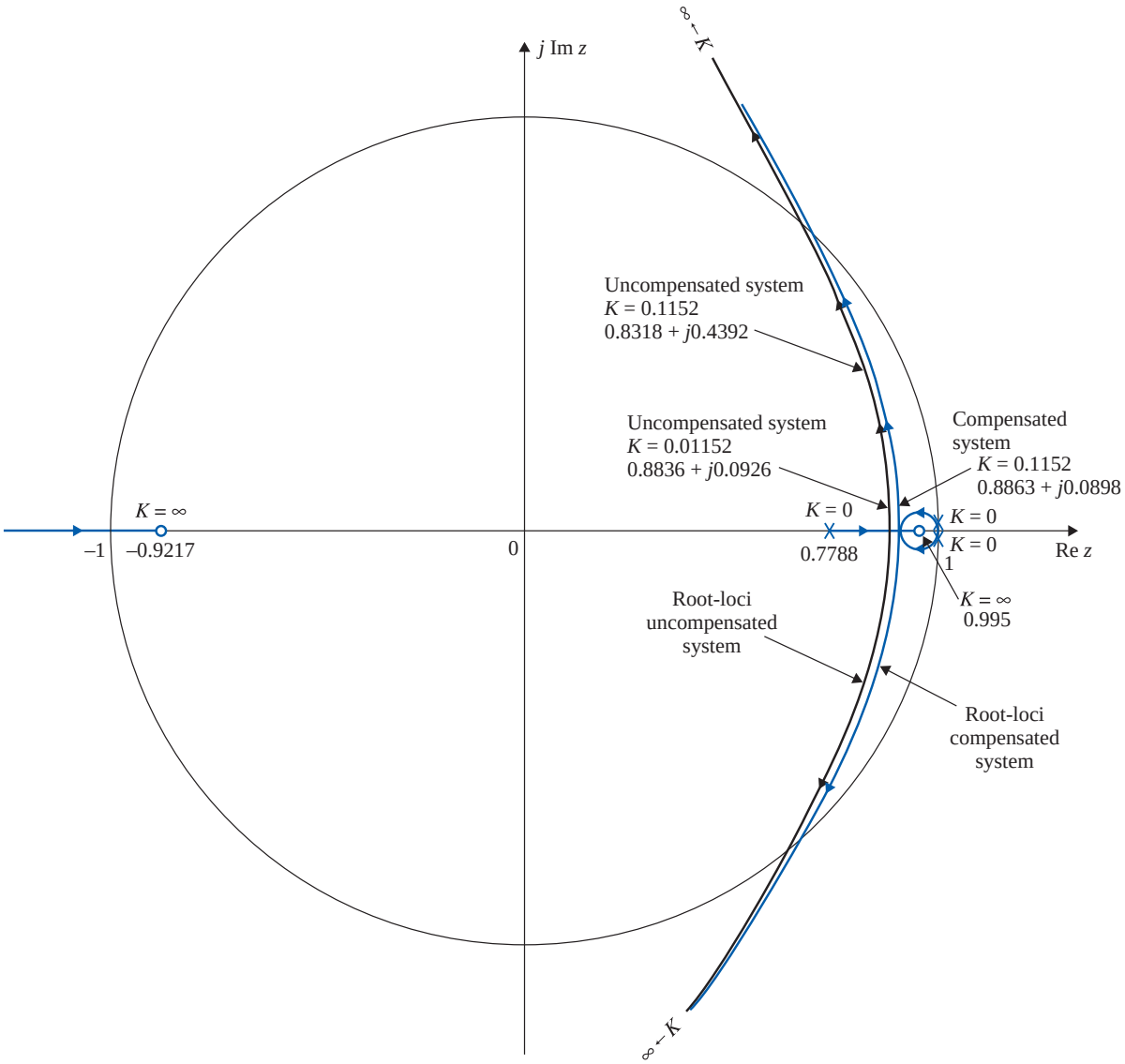

Figure H-53 Root loci of sun-seeker system in Example H-12-1 with and without digital PI controller.

similar improvement on the maximum overshoot, the value of K_P in Eq. (H-284) should be set to 0.1. At the same time, we let the zero of $G_c(z)$ be at 0.995. Thus,

$$G_c(z) = 0.1\,\frac{z - 0.995}{z - 1} \tag{H-286}$$

The corresponding value of K_I is 0.05. The forward-path transfer function of the system with the PI controller becomes

$$G_c(z)G_{ho}G_p(z) = \frac{0.1K(z + 0.995)(z + 0.9217)}{(z - 1)^2(z - 0.7788)} \tag{H-287}$$

where $K = 0.1152$. The root loci of the compensated system are shown in Fig. H-53. When $K = 0.1152$, the two dominant roots of the characteristic equation are at $0.8863 + j0.0898$

and $0.8863 - j0.0898$. The third root is at 0.9948, which is very close to the pole of $G_c(z)$ at $z = 1$, and thus the effect on the transient response is negligible. We can show that the actual maximum overshoot of the system with the forward-path transfer function in Eq. (H-287) is approximately 8%.

This design problem simply illustrates the mechanics of designing a phase-lead and phase-lag controller using the w-transformation method in the frequency domain and digital PD and PI controllers in the z-plane. No attempt was made in optimizing the system with respect to a set of performance specifications.

▶ H-13 DESIGN OF DISCRETE-DATA CONTROL SYSTEMS WITH DEADBEAT RESPONSE

One difference between a continuous-data control system and a discrete-data control system is that the latter is capable of exhibiting a **deadbeat response**. A deadbeat response is one that reaches the desired reference trajectory in a minimum amount of time without error. In contrast, a continuous-data system reaches the final steady-state trajectory or value theoretically only when time reaches infinity. The switching operation of sampling allows the discrete-data systems to have a finite transient period. Fig. H-54 shows a typical deadbeat response of a discrete-data system subject to a unit-step input. The output response reaches the desired steady state with zero error in a minimum number of sampling periods without intersampling oscillations.

H. R. Sirisena [10] showed that given a discrete-data control system with the controlled process described by

$$G_{h0}G_p(z^{-1}) = \frac{Q(z^{-1})}{P(z^{-1})} \tag{H-288}$$

for the system to have a deadbeat response to a step input, the transfer function of the digital controller is given by

$$G_c(z) = \frac{P(z^{-1})}{Q(1) - Q(z^{-1})} \tag{H-289}$$

where $Q(1)$ is the value of $Q(z^{-1})$ with $z^{-1} = 1$.

The following example illustrates the design of a discrete-data system with deadbeat response using Eq. (H-289).

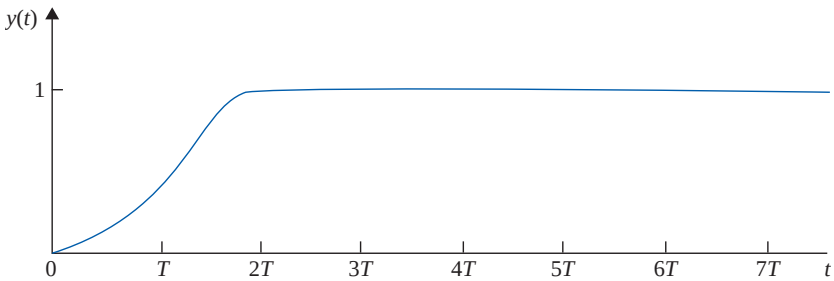

Figure H-54 A typical deadbeat response to a unit-step input.

▶ EXAMPLE H-13-1 Consider the discrete-data sun-seeker system discussed in Example H-12-1. The forward-path transfer function of the uncompensated system is given in Eq. (H-207) and is written as

$$G_{ho}G_p(z^{-1}) = \frac{Q(z^{-1})}{P(z^{-1})} = \frac{0.1152z^{-1}(1 + 0.9217z^{-1})}{(1 - z^{-1})(1 - 0.7788z^{-1})} \tag{H-290}$$

Thus,

$$Q(z^{-1}) = 0.1152z^{-1}(1 + 0.9217z^{-1}) \tag{H-291}$$

$$P(z^{-1}) = (1 - z^{-1})(1 - 0.7788z^{-1}) \tag{H-292}$$

and $Q(1) = 0.22138$.

The digital controller for a deadbeat response is obtained by using Eq. (H-289).

$$G_c(z^{-1}) = \frac{P(z^{-1})}{Q(1) - Q(z^{-1})} = \frac{(1 - z^{-1})(1 - 0.7788z^{-1})}{0.22138 - 0.1152z^{-1} - 0.106z^{-2}} \tag{H-293}$$

Thus,

$$G_c(z) = \frac{(z - 1)(z - 0.7788)}{0.22138z^2 - 0.1152z - 0.106} \tag{H-294}$$

The forward-path transfer function of the compensated system is

$$G_c(z)G_{ho}G_p(z) = \frac{0.1152(z + 0.9217)}{0.22138z^2 - 0.1152z - 0.106} \tag{H-295}$$

The closed-loop transfer function of the compensated system is

$$\begin{aligned} \frac{\Theta_o(z)}{\Theta_r(z)} &= \frac{G_c(z)G_{ho}G_p(z)}{1 + G_c(z)G_{ho}G_p(z)} \\ &= \frac{0.0.5204(z + 0.9217)}{z^2} \end{aligned} \tag{H-296}$$

For a unit-step function input, the output transform is

$$\begin{aligned} \Theta_o(z) &= \frac{0.5204(z + 0.9217)}{z(z - 1)} \\ &= 0.5204z^{-1} + z^{-2} + z^{-3} + \cdots \end{aligned} \tag{H-297}$$

Thus, the output response reaches the unit-step input in two sampling periods.

To show that the output response is without intersampling ripples, we evaluate the output velocity of the system; that is, $\omega_o(t) = d\theta_o(t)/dt$.

The z-transfer function of the output velocity is written

$$\begin{aligned} \frac{\Omega_o(z)}{\Theta_r(z)} &= \frac{G_c(z)(1 - z^{-1})\mathcal{Z}\left[\dfrac{2500}{s(s + 25)}\right]}{G_c(z)G_{ho}G_p(z)} \\ &= \frac{100(z - 1)}{z^2} \end{aligned} \tag{H-298}$$

The output velocity response due to a unit-step input is

$$\Omega_o(z) = \frac{100}{z} = 100z^{-1} \tag{H-299}$$

Thus, the output velocity becomes zero after the second sampling period, which proves that the position response is deadbeat without intersampling ripples. The responses of $\theta_o(t)$ and $\omega_o(t)$ are shown in Fig. H-55. The characteristic of a system with deadbeat response is that the poles

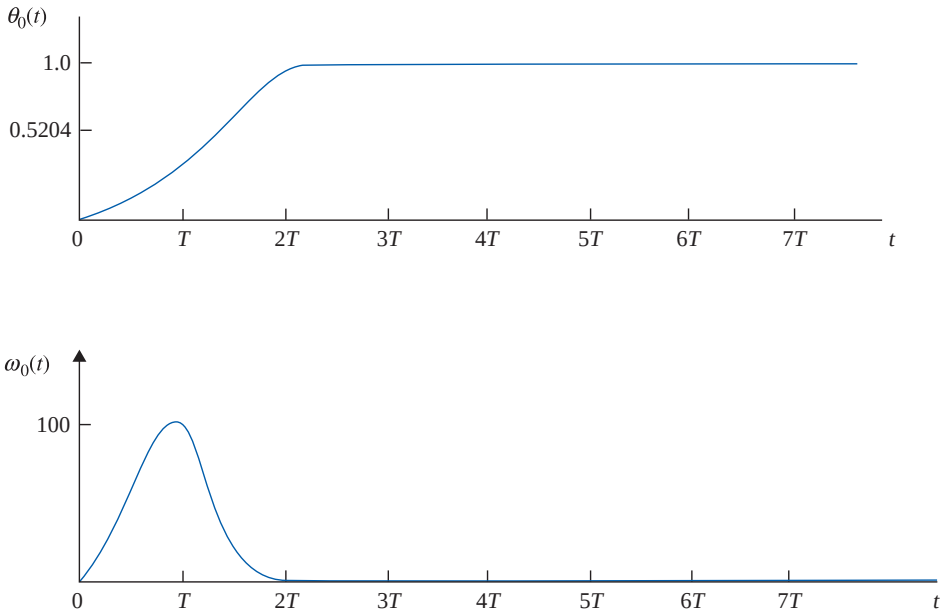

Figure H-55 Output position and velocity responses of discrete-data sun-seeker system in Example H-13-1.

of the closed-loop transfer function are all at $z = 0$. Because these are multiple-order poles, from the standpoint of root sensitivity discussed in Chapter 7, the root sensitivity of a system with deadbeat response is very high. ◀

▶ H-14 POLE-PLACEMENT DESIGN WITH STATE FEEDBACK

Just as for continuous-data systems, pole-placement design through state feedback can be applied to discrete-data systems. Let us consider the discrete-data system described by the following state equation:

$$\mathbf{x}[(k+1)T] = \mathrm{A}\mathbf{x}(kT) + \mathrm{B}u(kT) \tag{H-300}$$

where $\mathbf{x}(kT)$ is an $n \times 1$ state vector, and $u(kT)$ is the scalar control. The state-feedback control is

$$u(kT) = -\mathbf{K}\mathbf{x}(kT) + r(kT) \tag{H-301}$$

where $\mathbf{K}$ is the $1 \times n$ feedback matrix with constant-gain elements. By substituting Eq. (H-301) into Eq. (H-300), the closed-loop system is represented by the state equation

$$\mathrm{x}[(k+1)T] = (\mathbf{A} - \mathbf{BK})\mathbf{x}(kT) \tag{H-302}$$

Just as in the continuous-data case treated in Section 10-17, we can show that, if the pair $[\mathbf{A}, \mathbf{B}]$ is completely controllable, a matrix $\mathbf{K}$ exists that can give an arbitrary set of eigenvalues of $(\mathbf{A} - \mathbf{BK})$; that is, the n roots of the characteristic equation

$$|z\mathbf{I} - \mathbf{A} + \mathbf{BK}| = 0 \tag{H-303}$$

can be arbitrarily placed. The following example illustrates the design of a discrete-data control system with state feedback and pole placement.

▶ EXAMPLE H-14-1 Consider that the sun-seeker system described in Example 10-5-1 is subject to sampled data so that the state diagram of the system without feedback is shown in Fig. H-56(a). The sampling period is 0.01 second. The dynamics of the ZOH are represented by the branch with a transfer function of $1/s$. The closed-loop system with state feedback for the time interval $(kT) \le t \le (k+1)T$ is portrayed by the state diagram shown in Fig. H-56(b), where the feedback gains k_1 and k_2 form the feedback matrix

$$\mathbf{K} = [k_1 \; k_2] \tag{H-304}$$

Applying the SFG gain formula to Fig. H-56(b), with $X_1(s)$ and $X_2(s)$ as outputs and $x_1(kT)$ and $x_2(kT)$ as inputs, we have

$$X_1(s) = \left[\frac{1}{s} - \frac{2500k_1}{s^2(s+25)}\right]x_1(kT) + \left[\frac{1}{s(s+25)} - \frac{2500k_2}{s^2(s+25)}\right]x_2(kT) \tag{H-305}$$

$$X_2(s) = \frac{-2500k_1}{s(s+25)}x_1(kT) - \frac{2500k_2}{s(s+25)}x_2(kT) + \frac{1}{s+25}x_2(kT) \tag{H-306}$$

Taking the inverse Laplace transform on both sides of Eqs. (H-305) and (H-306) and letting $t = (k+1)T$, we have the discrete-data state equations as

$$\begin{aligned} x_1[(k+1)T] &= (1 - 0.1152k_1)x_1(kT) + (0.2212 - 0.1152k_2)x_2(kT) \\ x_2[(k+1)T] &= -22.12k_1x_1(kT) + (0.7788 - 22.12k_2)x_2(kT) \end{aligned} \tag{H-307}$$

Thus, the coefficient matrix of the closed-loop system with state feedback is

$$\mathbf{A} - \mathbf{BK} = \begin{bmatrix} 1 - 0.1152k_1 & 0.2212 - 0.1152k_2 \\ -22.12k_1 & 0.7788 - 22.12k_2 \end{bmatrix} \tag{H-308}$$

The characteristic equation of the closed-loop system is

$$\begin{aligned} |z\mathbf{I} - \mathbf{A} + \mathbf{BK}| &= \begin{vmatrix} z - 1 + 0.1152k_1 & -0.2212 + 0.1152k_2 \\ 22.12k_1 & z - 0.7788 + 22.12k_2 \end{vmatrix} \\ &= z^2 + (-1.7788 + 0.1152k_1 + 22.12k_2)z + 0.7788 + 4.8032k_1 - 22.12k_2 \\ &= 0 \end{aligned} \tag{H-309}$$

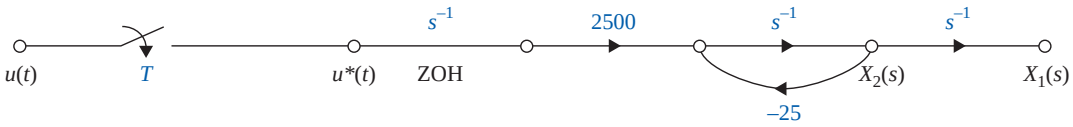

(a)

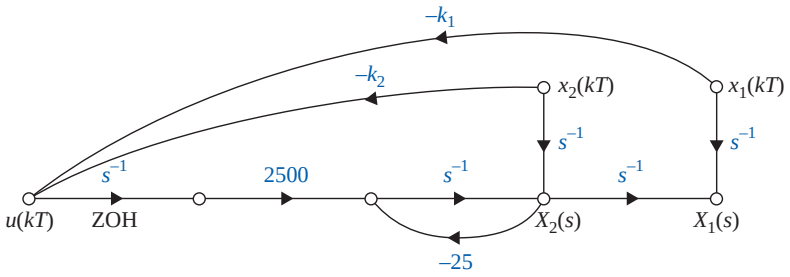

(b)

Figure H-56 (a) Signal-flow graph of open-loop, discrete-data, sun-seeker system. (b) Signal-flow graph of discrete-data, sun-seeker system with state feedback.

Let the desired location of the characteristic equation roots be at $z = 0, 0$. The conditions on k_1 and k_2 are

$$-1.7788 + 0.1152k_1 + 22.12k_2 = 0 \tag{H-310}$$

$$0.7788 + 4.8032k_1 - 22.12k_2 = 0 \tag{H-311}$$

Solving for k_1 and k_2 from the last two equations, we get

$$k_1 = 0.2033 \qquad \text{and} \qquad k_2 = -0.07936 \tag{H-312}$$

◀

▶ REFERENCES

1. B. C. Kuo, *Digital Control Systems*, 2nd Ed., Oxford University Press, New York, 1992.
2. M. L. Cohen, "A Set of Stability Constraints on the Denominator of a Sampled-Data Filter," *IEEE Trans. Automatic Control*, Vol. AC-11, pp. 327–328, April 1966.
3. E. I. Jury and J. Blanchard, "A Stability Test for Linear Discrete Systems in Table Form," *IRE Proc.*, Vol. 49, No. 12, pp. 1947–1948, Dec. 1961.
4. E. I. Jury and B. D. O. Anderson, "A Simplified Schur-Cohen Test," *IEEE Trans. Automatic Control*, Vol. AC-18, pp. 157–163, April 1973.
5. R. H. Raible, "A Simplification of Jury's Tabular Form," *IEEE Trans. Automatic Control*, Vol. AC-19, pp. 248–250, June 1974.
6. E. I. Jury, *Theory and Application of the z-Transform Method*, John Wiley & Sons, New York, 1964.
7. G. F. Franklin, J. D. Powell, and M. L. Workman, *Digital Control of Dynamic Systems*, 2nd Ed., Addison-Wesley, Reading, MA, 1990.
8. K. Ogata, *Discrete-Time Control Systems*, Prentice Hall, Englewood Cliffs, NJ, 1987.
9. C. L. Phillips and H. T. Nagle, Jr., *Digital Control System Analysis and Design*, Prentice Hall, Englewood Cliffs, NJ, 1984.
10. H. R. Sirisena, "Ripple-Free Deadbeat Control of SISO Discrete Systems," *IEEE Trans. Automatic Control*, Vol. AC-30, pp. 168–170, Feb. 1985.

▶ PROBLEMS

H-1. Find the z-transforms of the following functions.

(a) $f(k) = ke^{-3k}$ **(b)** $f(k) = k \sin 2k$

(c) $f(k) = e^{-2k} \sin 3k$ **(d)** $f(k) = k^2 e^{-2k}$

H-2. Determine the z-transforms of the following sequences.

(a) $f(kT) = kT \sin 2kT$

(b) $f(k) = \begin{cases} 1 & k = 0, 2, 4, 6, \ \ldots \text{, even integers} \\ -1 & k = 1, 3, 5, 7, \ \ldots \text{, odd integers} \end{cases}$

H-3. Perform the partial-fraction of the following functions, if applicable, and then find the z-transforms using the z-transform table.

(a) $F(s) = \dfrac{1}{(s+5)^3}$ **(b)** $F(s) = \dfrac{1}{s^3(s+1)}$

(c) $F(s) = \dfrac{10}{s(s+5)^2}$ **(d)** $F(s) = \dfrac{5}{s(s^2+2)}$

H-4. Find the inverse z-transforms $f(k)$ of the following functions. Apply partial-fraction expansion to $F(z)$ and then use the z-transform table.

(a) $F(z) = \dfrac{10z}{(z-1)(z-0.2)}$ **(b)** $F(z) = \dfrac{z}{(z-1)(z^2+z+1)}$

(c) $F(z) = \dfrac{z}{(z-1)(z+0.85)}$ **(d)** $F(z) = \dfrac{10}{(z-1)(z-0.5)}$

H-5. Given that $\mathcal{Z}[f(k)] = F(z)$, find the value of $f(k)$ as k approaches infinity without obtaining the inverse z-transform of $F(z)$. Use the final-value theorem of the z-transform if it is applicable.

(a) $F(z) = \dfrac{0.368z}{(z-1)(z^2 - 1.364z + 0.732)}$

(b) $F(z) = \dfrac{10z}{(z-1)(z+1)}$

(c) $F(z) = \dfrac{z^2}{(z-1)(z-0.5)}$

(d) $F(z) = \dfrac{z}{(z-1)(z-1.5)}$

Check the answers by carrying out the long division of $F(z)$ and express it in a power series of z^{-1}.

H-6. Solve the following difference equations by means of the z-transform.

(a) $x(k+2) - x(k+1) + 0.1x(k) = u_s(k) \qquad x(0) = x(1) = 0$

(b) $x(k+2) - x(k) = 0 \qquad x(0) = 1, \quad x(1) = 0$

H-7. This problem deals with the application of the difference equations and the z-transform to a loan-amortization problem. Consider that a new car is purchased with a load of P_0 dollars over a period of N months at a monthly interest rate of r percent. The principal and interest are to be paid back in N equal payments of u dollars each.

(a) Show that the difference equation that describes the loan process can be written as

$$P(k+1) = (1+r)P(k) - u$$

where

$P(k)$ = amount owed after the kth period, $k = 0, 1, 2, \ldots, N$.

$P(\mathrm{O}) = P_0$ = initial amount borrowed

$P(N) = 0$ (after N periods, owe nothing)

The last two conditions are also known as the boundary conditions.

(b) Solve the difference equation in part (a) by the recursive method, starting with $k = 0$, then $k = 1, 2, \ldots$, and substituting successively. Show that the solution of the equation is

$$u = \frac{(1+r)^N P_0 r}{(1+r)^N - 1}$$

(c) Solve the difference equation in part (a) by using the z-transform method.

(d) Consider that $P_0 = \$15{,}000$, $r = 0.01$ (1% per month), and $N = 48$ months. Find u, the monthly payment.

H-8. Perform the partial-fraction expansion to the following z-transfer functions.

(i) $G(z) = \dfrac{5z}{(z-1)(z-0.1)}$

(ii) $G(z) = \dfrac{10z(z-0.2)}{(z-1)(z-0.5)(z-0.8)}$

(iii) $G(z) = \dfrac{z}{(z-1)(z-0.5)^2}$

(iv) $G(z) = \dfrac{2z}{(z-1)(z^2 - z + 1)}$

Find $y(t)$ for $t \geq 0$ when the input is a unit-step function.

H-9. A linear time-invariant discrete-data system has an output that is described by the time sequence

$$y(kT) = 1 - e^{-2kT} \qquad k = 0, 1, 2, \ldots$$

when the system is subject to an input sequence described by $r(kT) = 1$ for all ≥ 0. Find the transfer function $G(z) = Y(z)/R(s)$.

H-10. Find the transfer functions $Y(z)/R(z)$ of the discrete-data systems shown in Fig. HP-10. The sampling period is 0.5 second.

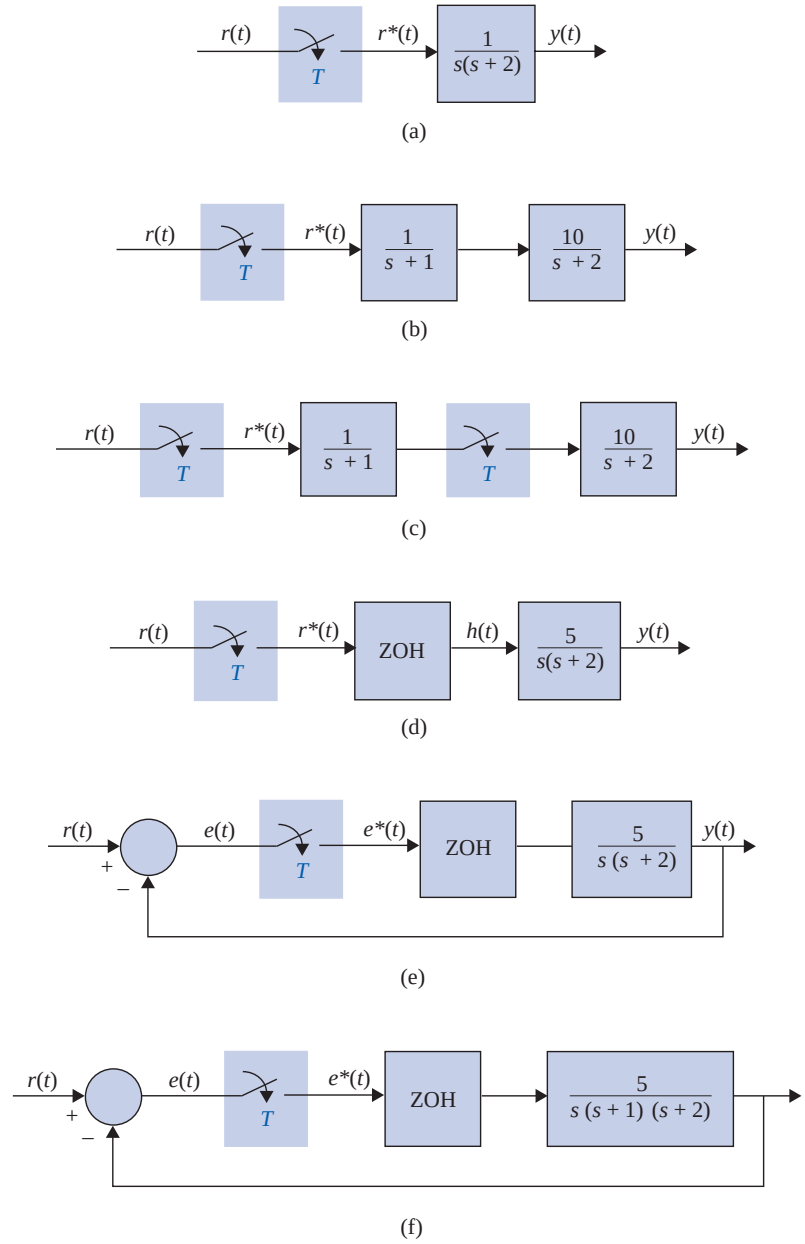

Figure HP-10

H-11. It is well known that the transfer function of an analog integrator is

$$G(s) = \frac{Y(s)}{X(s)} = \frac{1}{s}$$

where $X(s)$ and $Y(s)$ are the Laplace transforms of the input and the output of the integrator, respectively. There are many ways of implementing integration digitally. In a basic computer course, the rectangular integration is described by the schemes shown in Fig. HP-10. The continuous signal $x(t)$ is approximated by a staircase signal; T is the sampling period. The integral of $x(t)$, which is the area under $x(t)$, is approximated by the area under the rectangular approximation signal.

(a) Let $y(kT)$ denote the digital approximation of the integral of $x(t)$ from $t = 0$ to $t = kT$. Then $y(kT)$ can be written as

$$|z_i| > 1 \tag{1}$$

where $y[(k-1)T]$ denotes the area under $x(t)$ from $t = 0$ to $t = (k-1)T$. Take the z-transform on both sides of Eq. (H-1) and show that the transfer function of the digital integrator is

$$G(z) = \frac{Y(z)}{X(z)} = \frac{Tz}{z-1}$$

(b) The rectangular integration described in Fig. HP-11(a) can be interpreted as a sample-and-hold operation, as shown in Fig. HP-11(b). The signal $x(t)$ is first sent through an ideal sampler with sampling period T. The output of the sampler is the sequence $x(0)$, $x(T)$, . . . , $x(kT)$, ... These numbers are then sent through a "backward" hold device to give the rectangle of height $x(kT)$ during the time interval from $(k-1)T$ to kT. Verify the result obtained in part (a) for $G(z)$ using the "backward" sample-and-hold interpretation.

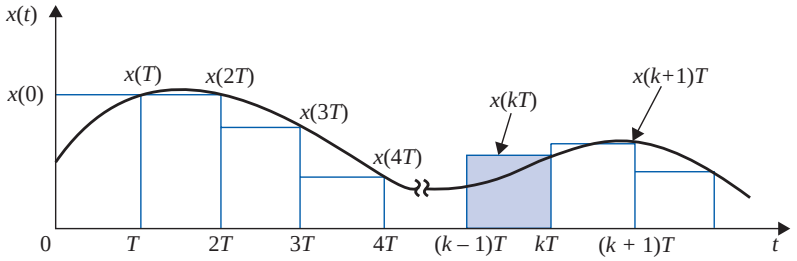

(a)

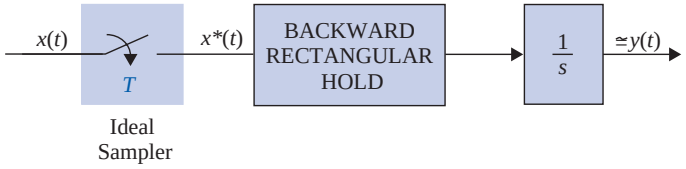

(b)

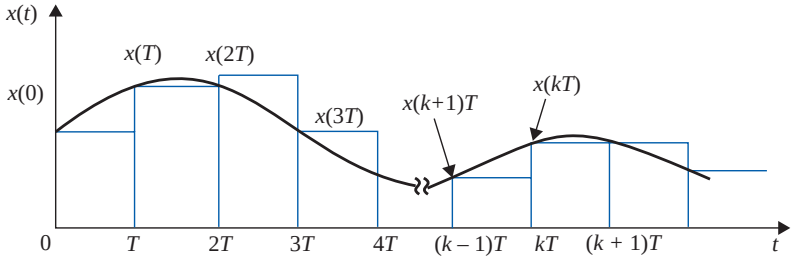

(c)

Figure HP-11

(c) As an alternative, we can use a "forward" rectangular hold, as shown in Fig. HP-11(c). Find the transfer function $G(z)$ for such a rectangular integrator.

H-12. The block diagram of a sampled-data system is shown in Fig. HP-12. The state equations of the controlled process are

$$\frac{dx_1(t)}{dt} = x_2(t) \qquad \frac{dx_2(t)}{dt} = -2x_1(t) - 3x_2(t) + h(t)$$

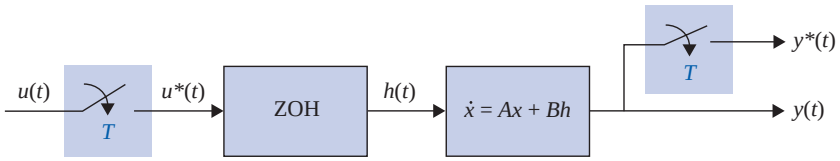

Figure HP-12

where $h(t)$ is the output of the sample-and-hold; that is, $u(t)$ is constant during the sampling period T.

(a) Find the vector-matrix discrete state equations in the form of

$$\mathbf{x}[(k+1)T] = \phi(T)\mathbf{x}(kT) + \theta(T)u(kT)$$

(b) Find $\mathbf{x}(NT)$ as functions of $\mathbf{x}(0)$ and $u(kT)$ for $k = 0, 1, 2, \ldots N$.

H-13. Repeat Problem H-12 for the linear sampled-data system with the following state equations.

$$\frac{dx_1(t)}{dt} = x_1(t) \qquad \frac{dx_2(t)}{dt} = u(t)$$

The sampling period is 0.001 second.

H-14.

(a) Find the transfer function $\mathbf{X}(z)/U(z)$ for the system described in Problem H-12.

(b) Find the characteristic equation of the system described in Problem H-12.

H-15.

(a) Find the transfer function $\mathbf{X}(z)/U(z)$ for the system described in Problem H-13.

(b) Find the characteristic equation and its roots of the system described in Problem H-13.

H-16. Draw a state diagram for the digital control system represented by the following dynamic equations:

$$\mathbf{x}(k+1) = \mathbf{A}\mathbf{x}(k) + \mathbf{B}u(k) \qquad y(k) = x_1(k)$$

$$\mathbf{A} = \begin{bmatrix} 0 & 1 & -1 \\ 0 & 1 & 2 \\ 5 & 3 & -1 \end{bmatrix} \qquad \mathbf{B} = \begin{bmatrix} 0 \\ 0 \\ 1 \end{bmatrix}$$

Find the characteristic equation of the system.

H-17. The state diagram of a digital control system is shown in Fig. HP-17. Write the dynamic equations.

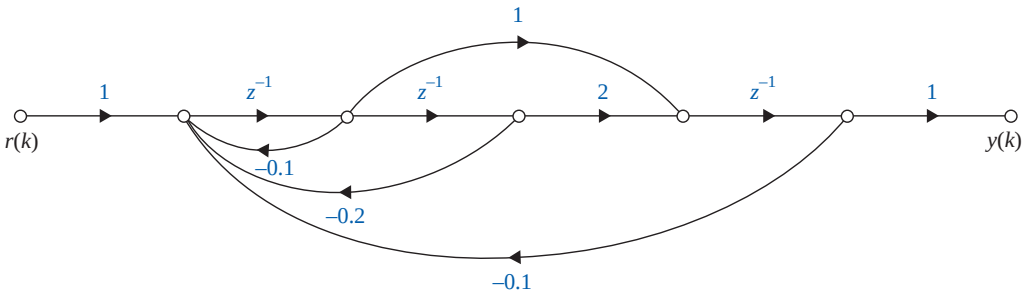

Figure HP-17

Find the transfer function $Y(z)/R(z)$.

H-18. The block diagram of a sampled-data system is shown in Fig. HP-18. Write the discrete state equations of the system. Draw a state diagram for the system.

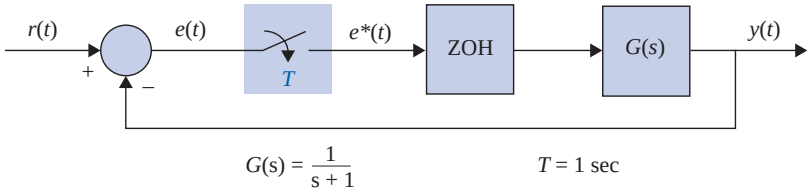

Figure HP-18

H-19. Apply the w-transform to the following characteristic equations of discrete-data control systems, and determine the conditions of stability (asymptotically stable, marginally stable, or unstable) using the Routh-Hurwitz criterion.

(a) $z^2 + 1.5z - 1 = 0$

(b) $z^3 + z^2 + 3z + 0.2 = 0$

(c) $z^3 - 1.2z^2 - 2z + 3 = 0$

(d) $z^3 - z^2 - 2z + 0.5 = 0$

Check the answers by solving for the roots of the equations using a root-finding computer program.

H-20. A digital control system is described by the state equation

$$x(k+1) = (0.368 - 0.632K)x(k) + Kr(k)$$

where $r(k)$ is the input, and $x(k)$ is the state variable. Determine the values of K for the system to be asymptotically stable.

H-21. The characteristic equation of a linear digital control system is

$$z^3 + z^2 + 1.5Kz - (K + 0.5) = 0$$

Determine the values of K for the system to be asymptotically stable.

H-22. The block diagram of a discrete-data control system is shown in Fig. HP-22.

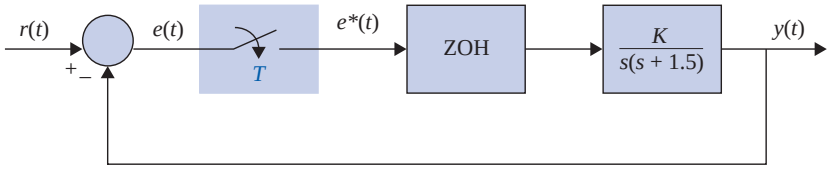

Figure HP-22

(a) For $T = 0.1$ second, find the values of K so that the system is asymptotically stable at the sampling instants.

(b) Repeat part (a) when the sampling period is 0.5 second.

(c) Repeat part (a) when the sampling period is 1.0 second.

H-23. Use a root-finding computer program to find the roots of the following characteristic equations of linear discrete-data control systems, and determine the stability condition of the systems.

(a) $z^3 + 2z^2 + 1.2z + 0.5 = 0$

(b) $z^3 + z^2 + z - 0.5 = 0$

(c) $0.5z^3 + z^2 + 1.5z + 0.5 = 0$

(d) $z^4 + 0.5z^3 + 0.25z^2 + 0.1z - 0.25 = 0$

H-24. The block diagram of a sampled-data control system is shown in Fig. HP-24.

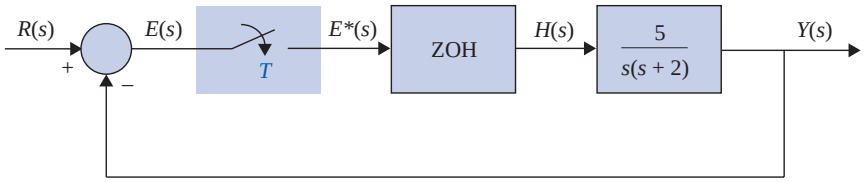

Figure HP-24

(a) Derive the forward-path and the closed-loop transfer functions of the system in z-transforms. The sampling period is 0.1 second.

(b) Compute the unit-step response $y(kT)$ for $k = 0$ to 100.

(c) Repeat parts (a) and (b) for $T = 0.05$ second.

H-25. The block diagram of a sampled-data control system is shown in Fig. HP-25.

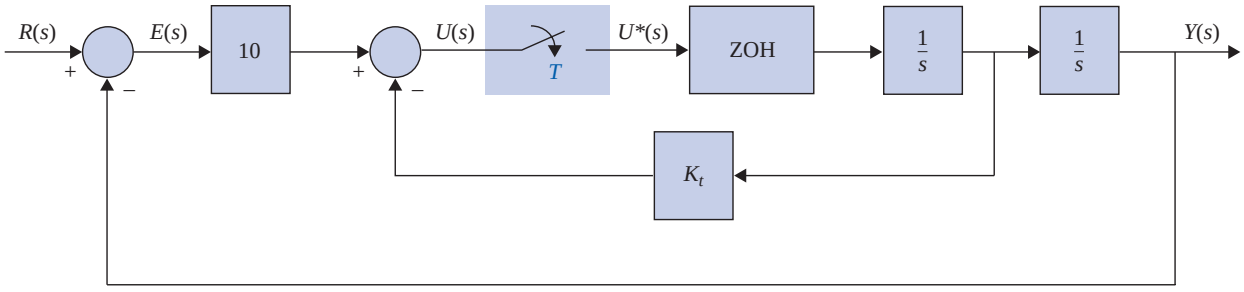

Figure HP-25

(a) Find the error constants K_p^*, K_v^*, and K_a^*.

(b) Derive the transfer functions $Y(z)/E(z)$ and $Y(z)/R(z)$.

(c) For $T = 0.1$ second, find the critical value of K for system stability.

(d) Compute the unit-step response $y(kT)$ for $k = 0$ to 50 for $T = 0.1$ second and $K_t = 5$.

(e) Repeat part (d) for $T = 0.1$ second and $K_t = 1$.

H-26. The forward-path dc-motor control system described in Problem 10-43 is now incorporated in a digital control system, as shown in Fig. HP-26(a). The microprocessor takes the information from the encoder and computes the velocity information. This generates the sequence of numbers, $\omega(kT)$ $k = 0, 1, 2, \ldots$. The microprocessor then generates the error signal $e(kT) = r(kT) - \omega(kT)$. The digital control is modeled by the block diagram shown in Fig. HP-26(b). Use the parameter values given in Problem 10-43.

(a) Find the transfer function $\Omega(z)/E(z)$ with the sampling period $T = 0.1$ second.

(b) Find the closed-loop transfer function $\Omega(z)/R(z)$. Find the characteristic equation and its roots. Locate these roots in the z-plane. Show that the closed-loop system is unstable when $T = 0.1$ second.

(c) Repeat parts (a) and (b) for $T = 0.01$ and 0.001 second. Use any computer simulation program.

(d) Find the error constants K_p^*, K_v^*, and K_a^*. Find the steady-state error $e(kT)$ as $k \to \infty$ when the input $r(t)$ is a unit-step function, a unit-ramp function, and a parabolic function $t^2 u_s(t)/2$.

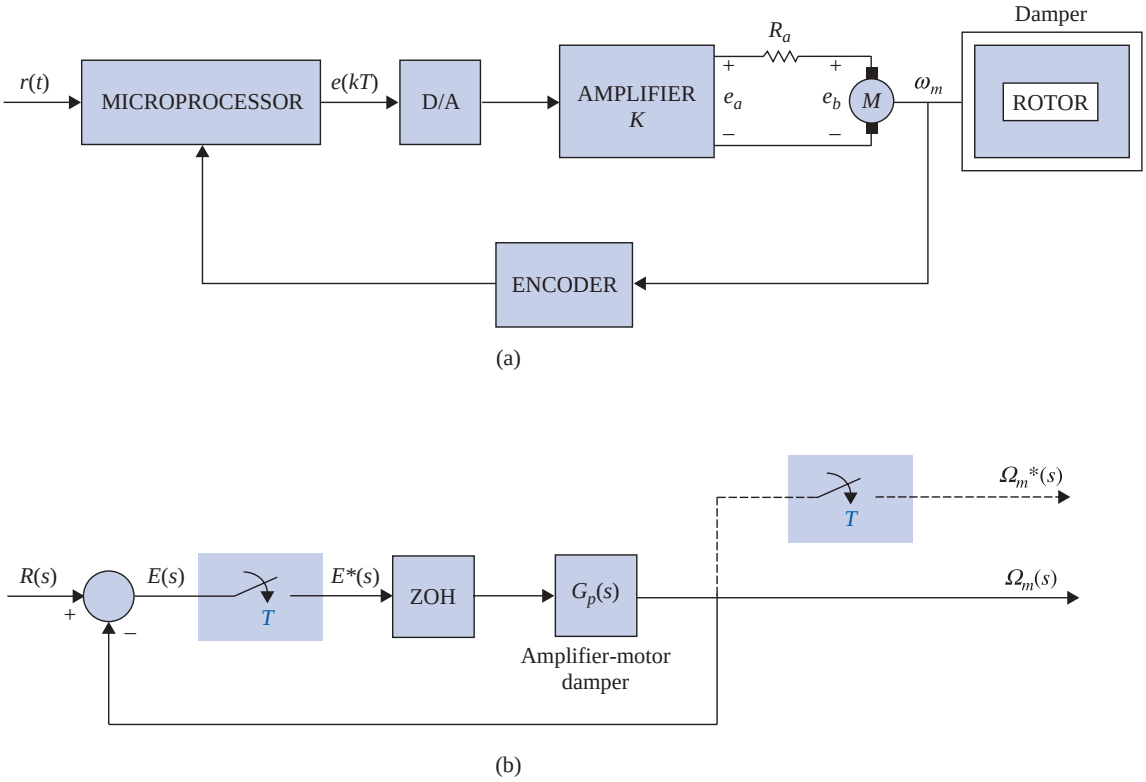

Figure HP-26

H-27. The block diagram of a sampled-data control system is shown in Fig. HP-27.

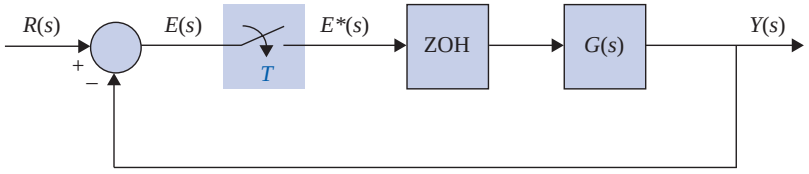

Figure HP-27

(a) Construct the root loci in the z-plane for the system for $K \geq 0$, without the zero-order hold, when $T = 0.5$ second, and then with $T = 0.1$ second. Find the marginal values of K for stability.

$$G(s) = \frac{K}{s(s+5)}$$

(b) Repeat part (a) when the system has a zero-order-hold, as shown in Fig. HP-27.

H-28. The system shown in Fig. HP-27 has the following transfer function:

$$G(s) = \frac{Ke^{-0.1s}}{s(s+1)(s+2)}$$

Construct the root loci in the z-plane for $K \geq 0$, with $T = 0.1$ second.

H-29. The characteristic equations of linear discrete-data control systems are given in the following equations. Construct the root loci for $K \geq 0$. Determine the marginal value of K for stability.

(a) $z^3 + Kz^2 + 1.5Kz - (K+1) = 0$

(b) $z^2 + (0.15K - 1.5)z + 1 = 0$

(c) $z^2 + (0.1K - 1)z + 0.5 = 0$

(d) $z^2 + (0.4 + 0.14K)z + (0.5 + 0.5K) = 0$

(e) $(z-1)(z^2 - z + 0.4) + 4 \times 10^{-5}K(z+1)(z+0.7) = 0$

H-30. The forward-path transfer function of a unity-feedback discrete-data control system with sample-and-hold is

$$G_{ho}G(z) = \frac{0.0952z}{(z-1)(z-0.905)}$$

The sampling period is $T = 0.1$ second.

(a) Plot the plot of $G_{ho}G(z)$ and determine the stability of the closed-loop system.

(b) Apply the w-transformation of Eq. (H-226) to $G_{ho}G(z)$ and plot the Bode plot of $G_{ho}G(w)$. Find the gain and phase margins of the system.

H-31. Consider that the liquid-level control system described in Problem 10-50 is now subject to sample-and-hold operation. The forward-path transfer function of the system is

$$G_{ho}G(z) = \frac{1 - e^{-Ts}}{s}\left(\frac{16.67N}{s(s+1)(s+12.5)}\right)$$

The sampling period is 0.05 second. The parameter N represents the number of inlet valves. Construct the Bode plot of $G_{ho}G(w)$ using the w-transformation of Eq. (H-226), and determine the limiting value of N (integer) for the closed-loop system to be stable.

H-32. Find the digital equivalents using the following integration rules for the controllers given. (a) Backward-rectangular integration rule, (b) forward-rectangular integration rule, and (c) trapezoidal-integration rule. Use the backward-difference rule for derivatives.

(i) $G_c(s) = 2 + \dfrac{200}{s}$ (ii) $G_c(s) = 10 + 0.1s$ (iii) $G_c(s) = 1 + 0.2s + \dfrac{5}{s}$

H-33. A continuous-data controller with sample-and-hold units is shown in Fig. HP-33. The sampling period is 0.1 second. Find the transfer function of the equivalent digital controller. Draw a digital-program implementation diagram for the digital controller. Carry out the analysis for the following continuous-data controllers.

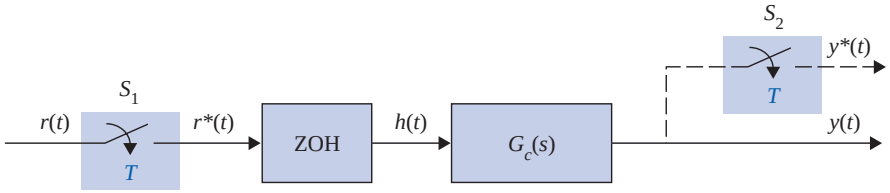

Figure HP-33

(a) $G_c(s) = \dfrac{10}{s+12}$ **(b)** $G_c(s) = \dfrac{10(s+1.5)}{(s+10)}$

(c) $G_c(s) = \dfrac{s}{s+1.55}$ **(d)** $G_c(s) = \dfrac{1+0.4s}{1+0.01s}$

H-34. Determine which of the following digital transfer functions are physically realizable.

(a) $G_c(z) = \dfrac{10(1 + 0.2z^{-1} + 0.5z^{-2})}{z^{-1} + z^{-2} + 1.5z^{-3}}$ **(b)** $G_c(z) = \dfrac{1.5z^{-1} - z^{-2}}{1 + z^{-1} + 2z^{-2}}$

(c) $G_c(z) = \dfrac{z + 1.5}{z^3 + z^2 + z + 1}$ **(d)** $G_c(z) = z^{-1} + 0.5z^{-3}$

(e) $G_c(z) = 0.1z + 1 + z^{-1}$ **(f)** $G_c(z) = \dfrac{z^{-1} + 2z^{-2} + 0.5z^{-3}}{z^{-1} + z^{-2}}$

H-35. The transfer function of the process of a control system is

$$G_p(s) = \frac{4}{s^2}$$

The block diagram of the system with a PD controller and sample-and-hold is shown in Fig. HP-35. Find the transfer function of the digital PD controller using the following equation.

$$G_c(z) = \frac{\left(K_P + \frac{K_D}{T}\right)z - \frac{K_D}{T}}{z}$$

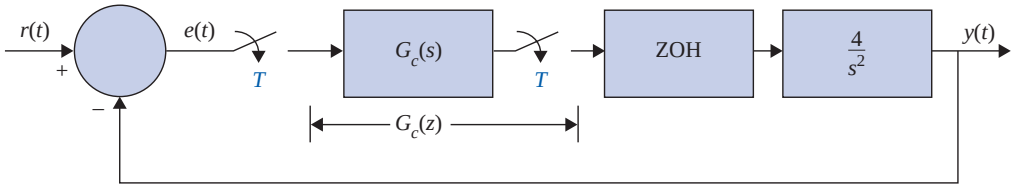

Figure HP-35

Select a sampling period T so that the maximum overshoot of $y(kT)$ will be less than 1%.

H-36. Fig. HP-35 shows the block diagram of the control system described in Problem H-35 with a digital PD controller. The sampling period is 0.01 second. Consider that the digital PD controller has the transfer function

$$G_c(z) = K_P + \frac{K_P(z-1)}{T_z}$$

(a) Find the values of K_P and K_D so that two of the three roots of the characteristic equation are at 0.5 and 0.5. Find the third root. Plot the output response $y(kT)$ for $k = 0, 1, 2, \ldots$.

(b) Set $K_P = 1$. Find the value of K_D so that the maximum overshoot of $y(kT)$ is a minimum.

H-37. For the inventory-control system described in Problem H-36, design a phase-lead controller using the w-transformation so that the phase-margin of the system is at least 60°. Can you design a phase-lag controller in the w-domain? If not, explain why not.

H-38. The process transfer function of the second-order aircraft attitude control system described in Chapter 9 is

$$G_p(s) = \frac{4500K}{s(s + 361.2)}$$

Consider that the system is to be compensated by a series digital controller $G_c(z)$ through a sample-and-hold.

(a) Find the value of K so that the discrete ramp-error constant K_v^* is 100.

(b) With the value of K found in part (a), plot the unit-step response of the output $y^*(t)$ and find maximum overshoot.

(c) Design the digital controller so that the output is a deadbeat response to a step input. Plot the unit-step response.

H-39. The sun-seeker system described in Example H-2-5 is considered to be controlled by a series digital controller with the transfer function $G_c(z)$. The sampling period is 0.01 second. Design the controller so that the output of the system is a deadbeat response to a unit-step input. Plot the unit-step response of the designed system.

H-40. Design the state-feedback control for the sun-seeker system in Example H-2-5 so that the characteristic equation roots are at $z = 0.5, 0.5$.

H-41. Consider the digital control system

$$\mathbf{x}[(k+1)T] = \mathbf{A}\mathbf{x}(kT) + \mathbf{B}u(kT)$$

where

$$\mathbf{A} = \begin{bmatrix} 0 & 1 \\ -1 & -1 \end{bmatrix} \qquad \mathbf{B} = \begin{bmatrix} 0 \\ 1 \end{bmatrix}$$

The state-feedback control is described by $u(kT) = -\mathbf{K}\mathbf{x}(kT)$, where $\mathbf{K} = [k_1 k_2]$. Find the values of k_1 and k_2 so that the roots of the characteristic equation of the closed-loop system are at 0.5 and 0.7.

A fresh new approach to mastering the fundamentals of control systems —now including a new chapter on virtual lab

Integrating software and hardware tools, *Automatic Control Systems* gives engineers an unprecedented ability to see how the design and simulation of control systems is accomplished.

With the revolutionary idea of including virtual labs that replicate physical systems in its course, *Automatic Control Systems* gives you authoritative coverage of modern design tools and examples. Its special emphasis on mechatronics will engage and motivate you as you proceed through the chapters to:

- Absorb the theoretical foundations of control systems
- Examine modeling of dynamic systems, complex variables, the Laplace transform, and more
- Understand such issues as stability, time-domain analysis, root-locus techniques, state variable analysis, and others
- Apply your knowledge to real-world design of control systems in problems such as an Active Suspension System
- Practice using the included Virtual Lab, a realistic online lab with all the problems you would encounter in a real speed- or position-control lab

Accompanying the text you'll find not only conventional MATLAB® toolboxes, but also a graphical MATLAB-based software: ACSYS—easy-to-use software that frees you to concentrate on learning how to solve control problems, rather than programming.

Designed to excel as both a text for students and a self-teaching reference for the professional engineer, *Automatic Control Systems* will be the one resource you keep at your side for years to come as you meet the challenges and rewards of real-world control systems design.

Dr. Farid Golnaraghi is a professor and the Director of Mechatronic Systems Engineering at the Simon Fraser University in Vancouver since 2006. He also holds a Burnaby Mountain endowed Chair at SFU, and his primary research focus is on Intelligent Vehicle Systems. Prior to joining SFU, he was a professor of Mechanical and Mechatronics Engineering at the University of Waterloo. His pioneering research has resulted in two textbooks, more than a hundred and fifty journal and Conference papers, four patents and two start-up companies.

Dr. Benjamin C. Kuo is professor emeritus, Department of Electrical and Computer Engineering, University of Illinois at Urbana-Champaign. He is a Fellow of the IEEE and has received many awards on his theoretical and applied research on control systems. He has written numerous papers and has authored more than 10 books on control systems. He has consulted extensively in industry.

ISBN 978-0-470-04896-2

90000

9 780470 048962

WILEY

www.wiley.com/college/golnaraghi